MODELING MIRV FOOTPRINT CONSTRAINTS
IN THE WEAPONS ASSIGNMENT MODEL

THESIS

Elliot T. Fair, Major, USAF

DEPARTMENT OF THE AIR FORCE

AIR UNIVERSITY

AIR FORCE INSTITUTE OF TECHNOLOGY

Wright-Patterson Air Force Base, Ohio

DTIC QUALITY INSPECTED 1

1997O430 000

AFIT/GOA/ENS/97M-04

MODELING MIRV FOOTPRINT CONSTRAINTS
IN THE WEAPONS ASSIGNMENT MODEL

THESIS

Elliot T. Fair, Major, USAF

AFIT/GOA/ENS/97M-04

DISCLAIMER STATEMENT

The views expressed in this thesis are those of the author and do not reflect the official policy or position of the Department of Defense or the U. S. Government.

MODELING MIRV FOOTPRINT CONSTRAINTS
INTHE WEAPONS ASSIGNMENT MODEL

THESIS

Presented to the Faculty of the Graduate School of Engineering of the Air Force

Institute of Technology

Air University

In Partial Fulfillment of the

Requirements for the Degree of

Master of Science in Operations Research

Elliot T. Fair III, B.S., MAS

Major, USAF

MARCH 1997

THESIS APPROVAL

STUDENT: Elliot T. Fair III, Major, USAF   CLASS: GOA 97M
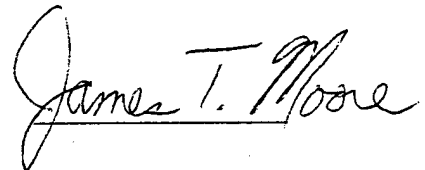
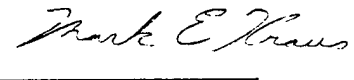THESIS TITLE: MODELING MIRV FOOTPRINT CONSTRAINTS
               IN THE WEAPONS ASSIGNMENT MODEL

DEFENSE DATE: 4 March 1997

COMMITTEE:	NAME/DEPARTMENT	SIGNATURE
Advisor	Lt Col James T. Moore/ENS	*James T. Moore*
Reader	Maj Mark E. Kraus/ENS	*Mark E. Kraus*

ACKNOWLEDGMENTS

Table of Contents

List of Figures

List of Figures (Continued)

List of Tables

List of Tables (Continued)

ABSTRACT

US Strategic Command (USSTRATCOM) is developing a new linear programming model called the Weapons Assignment Model (WAM) to perform weapons assignment for the Strategic Integrated Operations Plan (SIOP). One of the major improvements WAM will have over its predecessor is the ability to include Multiple Indepenently Targetable Reentry Vehicle (MIRV) footprinting constraints in the optimization process. In order to include MIRV footprint constraints in WAM, a methodology is needed to model the MIRV footprints in a manner that is consistent with the limitations of linear programming. Two techniques for modeling MIRV footprints were developed. The first, Geometric Approximation (GA), uses a carefully positioned and sized ellipse on the earth's surface to model the capabilities of a Post Boost Vehicle (PBV) to disperse MIRVs. Any combination of targets within the ellipse is considered to constitute a feasible targeting plan for a missile. The second model is called Energy Space Transformation (EST). This model scales the distance each MIRV is displaced from the missile aimpoint to account for the PBV energy required to maneuver for each MIRV. The sum of the maneuvering energy for each MIRV is used to calculate the fraction of the PBV energy required to strike a particular combination of targets. Any combination where the fraction is less than one is considered feasible. These two models were tested and verified using 120 missile sorties. Both models were approximately 85 percent accurate.

I. Introduction

Background

For years, America's nuclear war plans have been modeled using a preemptive goal programming model called the Arsenal Exchange Model (AEM). The algorithms in this model were designed under the restrictions of 1970's computer technology, which required the model to sacrifice exactness to reduce its computational complexity. One particular area in which AEM falls short is in the application of Multiple Independently Targetable Reentry Vehicle (MIRV) footprint constraints.

To address this and other shortcomings, the United States Strategic Command (USSTRATCOM) is developing a new linear programming model, the Weapons Assignment Model (WAM).

General Description of WAM

This section gives a general description of WAM, including differences between AEM and WAM, the required user inputs to WAM, and footprint constraints.

Improvements in WAM. The proposed model will differ from AEM in several respects. AEM allocates weapon types to target classes, whereas WAM will assign specific weapons to individual targets (9). This approach has several advantages. First, damage calculations will be more accurate because they can be made using the actual hardness of the individual targets, whereas AEM uses an

average hardness for each target in a target class. Second, better control of the allocation is afforded the user. This occurs since assigning weapons to individual targets facilitates greater segregation between attack options. Also, the user can apply weapon range limitations and known probabilities of arrival when specific targets are known (4).

WAM will also incorporate Designated Ground Zero (DGZ) selection into the optimization process. A DGZ is formed when more than one installation is to be attacked with the same warhead (5). WAM will create DGZs as it assigns weapons. Currently, DGZ construction and selection for AEM is done with a preprocessor prior to AEM execution (4). Thus, DGZ selection in AEM is not done as a part of the optimization process.

Finally, WAM will incorporate MIRV footprint constraints into the allocation process. AEM does not include the footprint constraints in its allocation process. Instead, AEM uses a heuristic after the allocation is complete that swaps weapons assignments to ensure footprint requirements are met. The subject of MIRV footprints is covered in more detail later. The development of MIRV footprint constraints that can be incorporated into the weapon allocation process is the thrust of this research.

Inputs. The inputs to WAM can be divided into two main categories - resources and goals. Resource inputs describe available weapons and potential targets. Available weapons include types of weapons, such as Peacekeeper warheads, B-1B gravity bombs, or Trident missile warheads. The input data

2

includes weapon parameters such as yield, reliability and number of MIRVs carried. Goals are objectives that the decision maker wants to be met. An example of a goal would be to achieve 90% damage expectancy (DE) against a particular class of targets, where DE reflects the probability of arrival of a weapon and the destructiveness of the weapon. Since the goals are assigned a priority which reflects their importance, WAM will use a preemptive goal programming formulation to ensure satisfaction of the different goals. The goals are dictated by force employment policies. The goal inputs are used to ensure the desired force employment is achieved. This is done by establishing a goal hierarchy, whereby the goal that is given highest priority will be met first, followed by satisfaction of the goal with the second highest priority, until all of the available resources are exhausted (4).

Footprint Constraints

Footprint constraints are constraints that account for the fact that MIRVs deployed from the same post boost vehicle (PBV) have certain geographic restrictions placed on their targets. Langley and Billings define a footprint as "a geometric figure whose size, shape, and orientation are dependent on the specific MIRV weapon system and launch site, and which defines an area of feasible coverage by a single MIRV (9:15)." These restrictions are due to the fact that a PBV has a limited amount of energy to use in dispersing its MIRVs. Therefore, the total sum of energy imparted to a set of MIRVs from a single PBV is bounded (9:8). This energy can be distributed in an infinite number of ways. For example,

3

all but one of the MIRVs can be targeted to a tight group of targets or DGZs,

while a single MIRV uses most of the PBV energy to strike a distant DGZ.

Alternatively, the energy could be distributed evenly to the MIRVs so they strike

evenly spaced DGZs. (9:8) These two concepts are illustrated in Figure 1-1.

All MIRVs given equal spacing

One MIRV uses most of the PBV energy
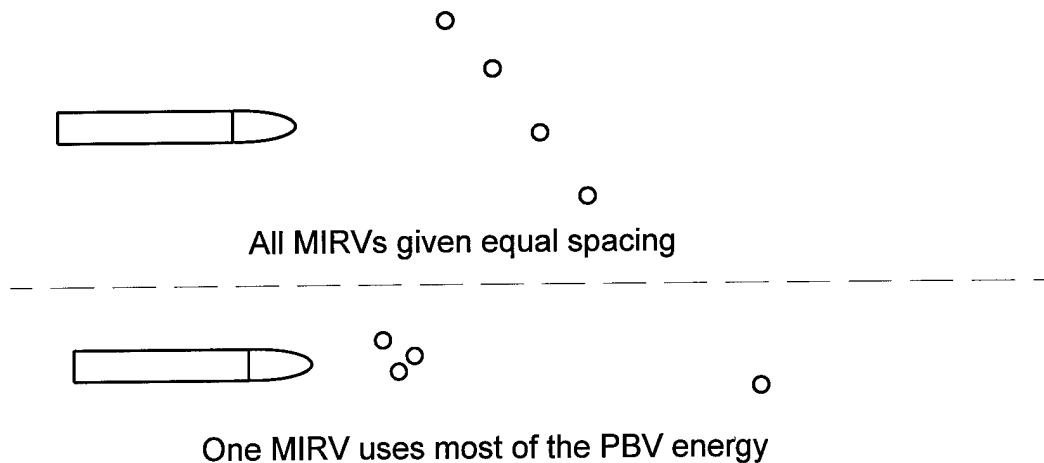
Figure 1-1. MIRV Distribution Options (9:9)

AEM does not include footprint constraints in its optimization process.

Instead, it arrives at a solution using preemptive goal programming which allows

MIRV targeting to be unrestricted. Once an allocation of all weapons is achieved,

a heuristic algorithm is used to swap MIRV/target combinations until all MIRVs

have realistic footprints (5). The heuristic uses a rectangular approximation of the

MIRV footprint. The rectangle is laid across a set of targets and any DGZ that

falls outside the rectangle is considered to be outside the footprint for that PBV.

DGZs are then traded between weapon systems until all DGZs fall within the

footprint for their respective PBV (6). This heuristic is used to assure feasibility,

4

but it does so without regard to the optimality of the solution. The result is a feasible solution that is no longer optimal.

Problem Definition

The Weapons Assignment Model will include MIRV footprint constraints in its formulation. The problem is to find a way to do this that permits the inclusion of the footprint constraints in a linear program. Thus, the purpose of this research is to develop an acceptable technique to model MIRV footprint constraints for the Weapons Assignment Model. The technique must be compatible with a linear programming formulation.

Scope

This thesis will focus only on the MIRV footprint constraints of WAM. For the purpose of finding a MIRV footprint model, an acceptable technique is defined as one that can replicate the results of a true footprint. The replication of the results does not have to be 100% correct in all cases, but it should be sufficiently accurate so as not to detract from the effectiveness of the solutions generated by the Weapons Assignment Model.

The footprinting methodology developed in this research is applicable only to missiles, and does not apply to the problem of footprinting bomber aircraft.

Format

Chapter II provides a more detailed description of the footprinting problem. The necessary background information to model MIRV footprints is presented.

Chapter III discusses two proposed models for the footprint constraints. These are

geometric approximation (GA) and energy space transformation (EST). The

methodology of the proposed models, including their formulation into linear

constraints, are presented in detail. In Chapter IV, the models are tested against a

missile simulation software package called Missile Performance System (MPS).

The models are developed and modified as necessary to produce acceptable

results. In Chapter V, the models are validated. Chapter VI presents conclusions

from the testing and makes recommendations.

II. Literature Review

Introduction

This chapter begins with a detailed description of the missile footprinting problem. The necessary background information on two proposed methods for incorporating the MIRV footprinting problem into a linear programming model is discussed in detail.

MIRV Footprints

Multiple independently targetable reentry vehicles (MIRVs) are carried aboard an assembly called a post boost vehicle (PBV). The PBV with the MIRVs attached is called a PBV assembly. The PBV assembly is carried aboard a missile and is released after the booster section has burned out. The PBV has its own limited maneuvering capability, which is used to properly align and position the MIRVs for a ballistic flight to their intended targets (10:9). Therefore, it is only through the maneuvering of the PBV that the MIRVs can gain separation from each other. Since the maneuvering capability of the PBV is limited, the allowable separation of the targets assigned to a PBV is also limited. The feasible area of coverage is the MIRV footprint (9:8). When several MIRVs are assembled on a PBV, a collective PBV footprint is produced. A PBV footprint can be thought of as a geographic region within which any pattern of MIRV laydown would be feasible. It is theoretically possible to compute every possible DGZ combination that could be feasibly struck by each PBV, but the number of calculations for a

7

problem with several thousand targets may be computationally prohibitive. For example, even if there were only 60 DGZs within range of a five MIRV system, there would be 5.5 million different DGZ combinations, each requiring a run of a missile simulation computer program to determine its feasibility. In actuality, the targets in range of US missile systems number in the thousands. Therefore, it is advantageous to approximate the true PBV footprint using a simple geometric figure whose size, shape, and orientation are carefully designed to enclose most feasible laydown patterns. However, since this is an approximation, there can be actual feasible laydown patterns where some DGZs fall outside the footprint approximation. For example, consider a weapon system configured with 10 MIRVs. The maximum distance that could be obtained between the missile focal point (the aim point of the PBV before any maneuvering energy is applied) and the furthest DGZ is obtained by allowing nine of the MIRVs to fall without expenditure of any PBV energy. The tenth MIRV then receives all of the PBV energy to extend its range in the direction of the missile flight path. Using a footprint approximation that is large enough to include the distant tenth DGZ would probably be too large to be useful in a model. This is because it is unlikely in the real world that the first nine MIRVs would not require any maneuvering energy, and if any of them use any energy at all, then ranging the tenth DGZ becomes infeasible. Thus, a useful footprint approximation would not necessarily contain every possible feasible MIRV laydown pattern.

It is also possible that a laydown pattern contained completely within the footprint approximation may be infeasible. This is primarily due to the issue of sequencing. (10:21) For example, consider the following set of DGZs.
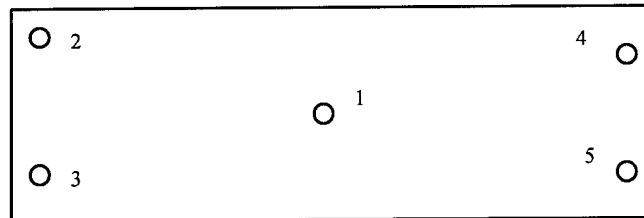
Figure 2-1. DGZ Set

The rectangular box represents a PBV footprint approximation. The PBV may be capable of striking all five DGZs in the order 1,2,3,4,5. However, it may not have the energy to strike the DGZs in a different sequence, such as 1,2,4,3,5. The second sequence would require a far greater amount of maneuvering energy to go from one end of the footprint to the other several times. To construct footprint approximations that are sufficiently small to prevent the possibility of including infeasible laydowns would produce footprints that are too small to be useful as they would rule out several feasible laydown strategies (6). Thus, a key to successfully modeling MIRV footprints is to properly define the size and shape of the footprint. The footprint size and shape are dependent on several factors.

Footprint size vs flight time. For each MIRV, the PBV adds a velocity vector to the one already imparted by the missile booster. For example, if the PBV adds to two MIRVs opposite velocity vectors lateral to the direction of the original velocity vector, then the MIRVs will continue to diverge for the

9

remainder of their flight time (10:15). MIRV separation perpendicular to the missile flight path is referred to as cross range. This is illustrated in the following figure.
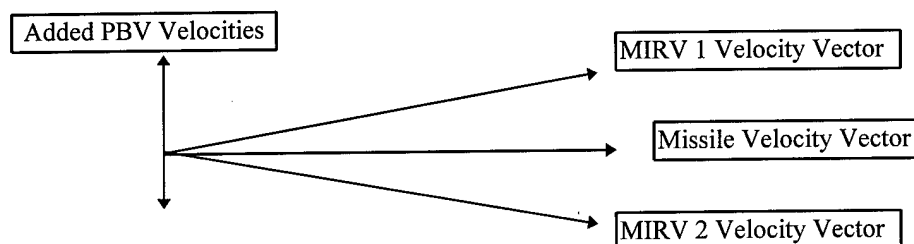
Figure 2-2. MIRV Cross Range Separation (10:11)

As the MIRV flight time increases, the dispersion between their respective impact points increases. Therefore, it is evident that the width of the MIRV footprint is dependent on the MIRV flight time.

The same logic can be applied to the length of the footprint. PBV energy can be applied to MIRVs to increase or decrease their range. MIRV dispersion along the missile flight path is referred to as down range. If two MIRVs are given different added velocities, X ft/sec and Y ft/sec, along the original flight path of the missile, then the impact points of the MIRVs differ along the axis of the missile flight path by a distance proportional to $(Y-X)^2$ and the difference in time of flight (4:11). Therefore, it can be seen that the footprint size in both the down range and cross range dimensions for a particular weapon system depend on the time of flight of the MIRVs for that system.

Factors affecting time of flight. There are three factors which affect the flight time of a MIRV. These are reentry envelope, range to target, and missile flight profile. Each warhead type has an acceptable reentry envelope that it must achieve in order to have a high probability of surviving reentry (10:12). This envelope is defined by a combination of reentry angle and reentry velocity. The acceptable reentry envelope, when plotted against the range to the first target, gives a window of possible flight times. The type of flight profile chosen for a particular missile sortie determines where in the window the flight time falls. An example of such a plot for a Poseidon missile armed with 10 Mk-3 MIRVs is given in Figure 2-3. The time of flight window in Figure 2-3 is labeled to show which flight profile applies to each area of the window. There are several flight profiles available that, combined with range, dictate the time of flight for a missile. The flight profiles are defined below.

MIRV Flight Profiles

Range extension. This profile is used for ranges at or near the limit of the system. On a range-extension profile, some or all of the PBV energy is given to a MIRV to extend its range.

Maximum loft. This profile is used for striking DGZs at the minimum range of a system. To accomplish a maximum-loft profile, the missile is fired on

TOF vs Range to First Target
(Poseidon 10 MIRV Configuration)
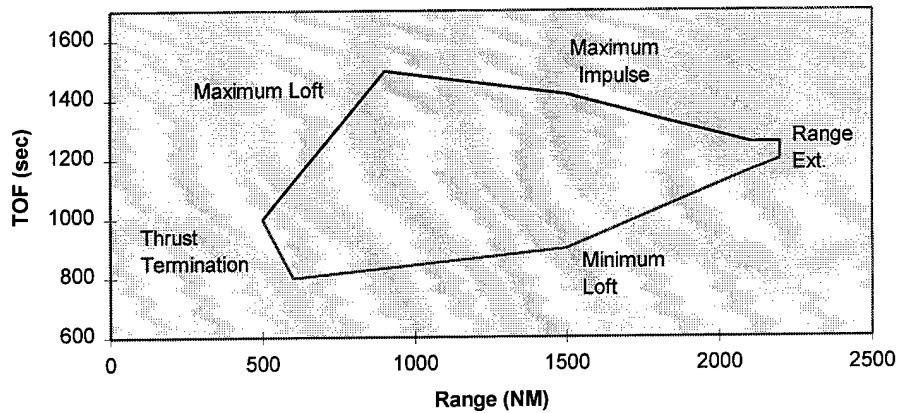
Figure 2-3. Missile Flight Profiles.

a maximum-loft trajectory, which is the steepest possible trajectory that can be used to hit the DGZ.

Some missiles, such as the Navy's Poseidon, have the capability of employing thrust termination (10:7). This means that the guidance systems in the booster can shut off the thrust prior to fuel exhaustion. Missiles with this capability can employ thrust termination on a maximum-loft profile in addition to the maximum-loft trajectory in order to strike short range DGZs.

Maximum impulse. Missiles on a maximum-impulse profile do not employ early thrust termination. The trajectory is decreased below the maximum-loft in order to increase range. This profile is used to position the PBV as far down range as possible.

Minimum loft. The minimum-loft profile is achieved by reducing the trajectory below that which would give maximum range. Early thrust termination is not employed.

Low angle thrust termination. This profile provides the shortest time of flight. It is used when the primary goal of the weapon is to strike DGZs that are time-sensitive. It is accomplished by using low trajectories combined with early thrust termination. This profile is available only for DGZs at the lower end of the range window (10:15).

As previously discussed, the size of the MIRV footprint is affected by the MIRV time of flight (TOF). It can be seen from Figure 2-3 that the MIRV TOF is dependent on the range and flight profile. Therefore, it stands to reason that the footprint size dependends on range and flight profile.

In practice, there are usually a myriad of feasible flight profiles for most DGZs except those at the system range limits or those with specific flight time requirements. For planning purposes, the flight profiles used can be classified into one of two general categories. Category I (TOF-I) profiles include all those that place the priority on maximizing the footprint size without regard to time of flight restrictions. These are represented by the top portion of the TOF window in Figure 2-3. Category II (TOF-II) profiles are those that place the priority on a short time of flight, regardless of how much the footprint size is reduced. These are represented by the bottom portion of Figure 2-3 (10:16).

Footprint Shape

To determine an effective geometric shape to use to model footprints, a comparison is needed between the down range distance and cross range distance a MIRV can be displaced given a unit of PBV energy. This can be done using the error analysis equations for missile targeting. The equation for down range targeting error, ΔR, for a unit change in velocity, ΔV, is: (12:81)

$$\Delta R/\Delta V = (2R_e/V)[\sin\theta_i + \cot\gamma(1-\cos\theta_i)] \qquad (2\text{-}1)$$

The equation for cross range targeting error, ΔL, for a unit change in velocity normal to the missile flight path, ΔV_n, is: (12:83)

$$\Delta L/\Delta V_n = (R_e/V)(\sin\theta_i/\cos\gamma) \qquad (2\text{-}2)$$

Where:

R_e = Radius of the earth, 6378.145 km

V = Velocity of the missile at burnout

θ_i = The range angle measured between launch point and impact point, with the origin at the center of the earth

γ = Flight path angle measured between the missile velocity vector and the local horizon

These equations are usually used to measure the miss distance caused by a velocity error at missile burnout, and are therefore based on the ΔV present at

burnout. However, when PBVs deploy MIRVs, they do so immediately after booster burnout both to confound enemy defenses and to achieve the maximum possible MIRV flight time in order to improve footprinting capability. Since the PBV ΔV is applied close to missile burnout, the above equations can be used as close approximations for the PBV ΔV required to achieve a certain MIRV displacement (14).

Consider equations (2-1) and (2-2) for a typical flight of an InterContinental Ballistic Missile (ICBM). Most US ICBMs are targeted for range angles close to 90 degrees (3:299). The velocity and flight path angle are not independent. In fact, there are an infinite number of pairs of (V, γ) that will achieve a given range angle (12:75). One way to select a value for γ is to assume an optimal (minimum velocity) trajectory. For an optimum trajectory, the optimum flight path angle, γ^*, can be found using

$$\gamma^* = (\pi/4) - (\theta_i/4) \quad (12:76) \tag{2-3}$$

which in this case gives $\gamma^* = 22.5$ degrees. A feasible (V, γ^*) pair can now be found by solving equation (2-4).

$$V^2 r_0/\mu = (1-\cos\theta_i)/[(r_0/R_e)\cos^2\gamma - \cos(\theta_i+\gamma)\cos\gamma] \quad (12:74) \tag{2-4}$$

where:

$\theta_i = 90^\circ$

$\gamma = 22.5^\circ$

r_o is the altitude at burnout measured from the center of the earth. (This is

usually very close to R_e and assumed to be the same) (12:81)

μ is a gravitational parameter equal to 1.4076×10^{16} ft³/sec² (3:429)

The burnout velocity V is found from equation (2-4) to be 7195 m/s. Substituting

values back into equation (2-1) gives $\Delta R/\Delta V \approx 6$ km/(m/s). Therefore, for a down

range PBV ΔV of 1 m/s, a MIRV will be displaced about 6 km. Converting units

gives a value of 0.9875 nm for a ΔV of 1 ft/sec. This is very close to the widely

accepted rule of thumb that a ΔV of 1 ft/sec in downrange equates to a 1 nm down

range displacement (3:305).

Using the same parameter values in equation (2-2) yields a $\Delta L/\Delta V_n$ value of

0.96 km/(m/s). This equates to a cross range displacement of 0.158 nm for a ΔV_n

of 1 ft/sec.

If the PBV has enough energy to supply a total ΔV of 1000 ft/sec, then a

single MIRV could be displaced a maximum of 1000 nm in down range or 158

nm in cross range. If a small ΔV is used in cross range, than the total down range

displacement would be slightly reduced. Conversely, any ΔV used for down

range displacement reduces the maximum cross range displacement that could be

achieved. Because of this trade-off relationship between the two axes, the shape

of the geographic area of coverage for a PBV is assumed to be elliptical (9:10).

This assumption was studied by the US Navy's MIRV Footprint Theory Study in 1974. After footprinting 128 missile sorties for the Strategic Integrated Operations Plan Revision L (SIOP REV L), a US nuclear war plan, a review of the results revealed that the DGZs were distributed in cross range and down range in a manner that suggested each footprint could be enclosed by an ellipse whose dimensions were proportional to the range from the missile launch point to the first DGZ (12:19). Comparisons between such ellipses and the DGZ set confirmed that the footprinting capability of a MIRVed missile can be approximated using an ellipse. In addition, high-fidelity mathematical models that analyze each event of a missile's flight were used to footprint the same sorties. The footprints produced from these models were compared to the elliptical approximations. The results showed that it was possible to select the dimensions of the ellipses such that they enclosed all of the DGZs of feasible sorties 98% of the time (10:21). A sortie is defined as a specific mission including a designated missile system, number of MIRVs, launch site, missile aim point, and order of DGZs to be struck.

Modeling Footprint Size

Determining the appropriate size of the footprint ellipse is pivotal to successfully modeling MIRV footprints. One way this problem has been successfully approached is through the use of stick lengths. A stick length is

defined as the geographic distance from the first MIRV impact point to the last

MIRV impact point, where all of the PBV energy is expended and all of the DGZs

are equally spaced. Stick lengths can be measured in either cross range or

down range. Figure 2-4 depicts the stick lengths.
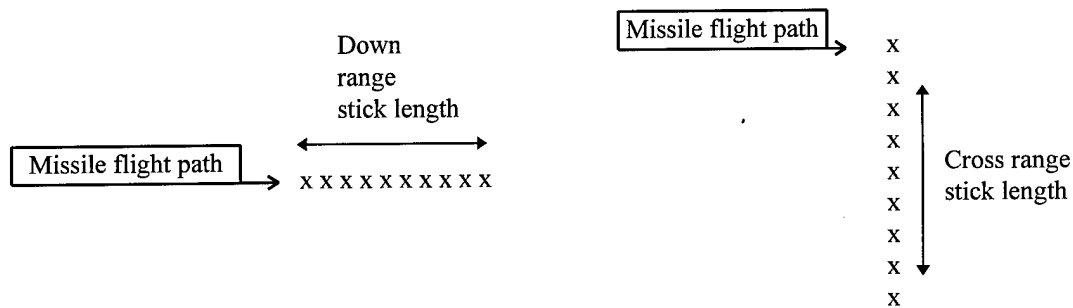
FIGURE 2-4. Down Range and Cross Range Stick Length (10:16-17)

Note that the two stick lengths are mutually exclusive. In other words, achieving

the down range stick length means no PBV energy remains for cross range

displacement.

The sizes of the stick lengths are dependent on the same factors that affect

footprint size. Plots for cross range and down range stick lengths are given in

Figures 2-5 and 2-6 for a Poseidon missile armed with 10 Mk-3 MIRVs. Data is

provided for both TOF-I and TOF-II trajectories. Figures 2-5 and 2-6 show down

range stick length versus range-to-first-target and cross range stick length versus

range-to-first-target, respectively. Note the direct relationship between stick

length and range-to-first-target for TOF-I trajectories.

Down Range Stick Length vs Range

Stick length (NM) vs Range to first target (NM)
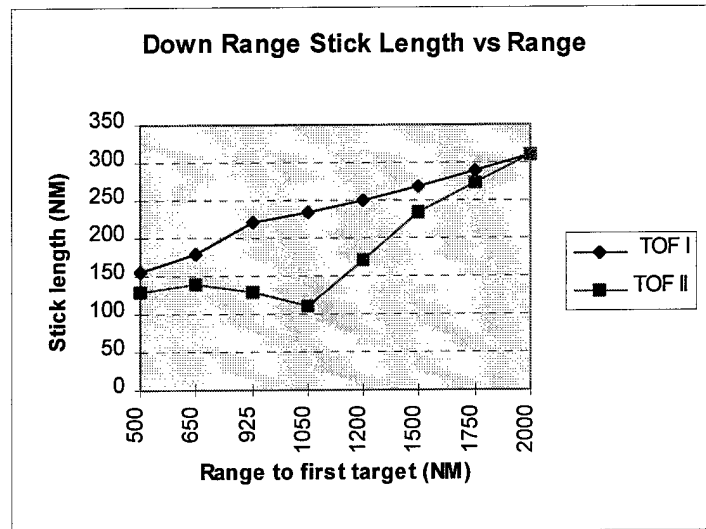
FIGURE 2-5. Down Range Stick Length vs Range

Cross Range Length vs Range

Stick Length (NM) vs Range to First Target (NM)
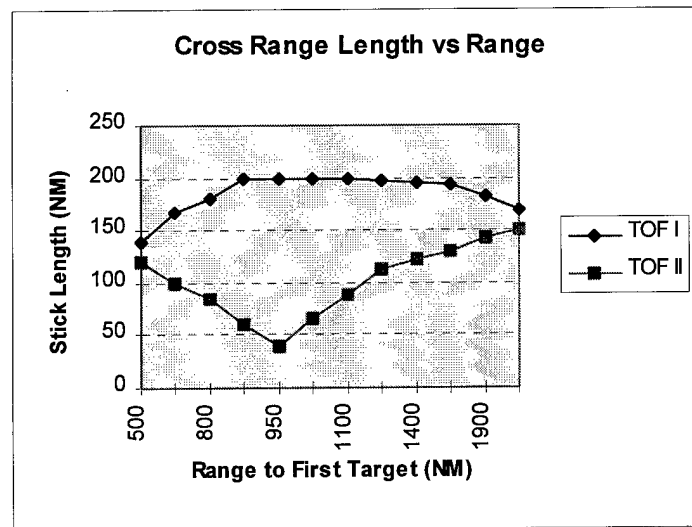
FIGURE 2-6. Cross Range Stick Length vs Range

Due to the equations of motion for high trajectory flight profiles, the error

terms for these profiles are generally smaller than for low trajectory flight

profiles. This means better accuracy is achieved when high trajectory, or TOF-I

profiles are used. For this reason, plus the added flexibility given by larger footprints, the majority of US missiles are planned on high trajectory profiles (3:305). A US Navy study done in 1974 on SIOP REV N found that of 320 Poseidon missiles targeted, 92% were planned for maximum or near maximum time of flight trajectories. The remaining missiles were planned somewhere in the middle of Figure 2-3, and none were planned at the absolute minimum TOF trajectory (10:20-21). For these reasons, it is assumed from this point on that all missiles are using a high profile maximum TOF trajectory. Figure 2-7 combines the TOF-I trajectory stick length data for both cross range and down range.
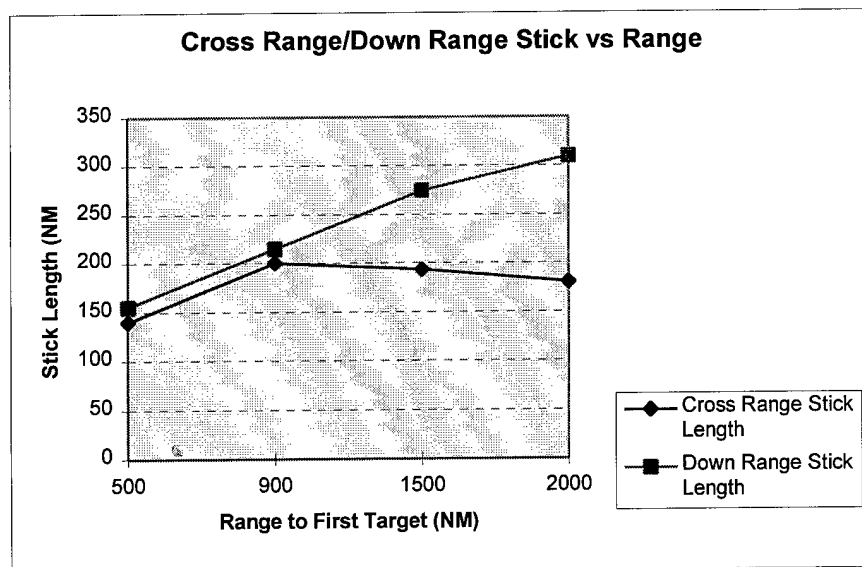
FIGURE 2-7. Cross/Down Range Stick Lengths vs Range-to-First-Target

Summary

Because MIRVs are dispersed by a PBV whose energy is limited, the footprint in which the PBV can disperse the MIRVs is limited. The size of the

footprint is primarily dependent on the time of flight of the missile system, which can be modeled with range. An ellipse provides an accurate and conveniant geographic figure to model footprints.

Based on this information, the methodology for implementing MIRV footprint models can now be developed. Chapter III presents two such models, the geometric approximation model and the energy space transformation model.

III. Methodology

Introduction

In this chapter, the theory is developed for an energy space transformation model and a geometric approximation model. Then the methodology to apply the models is presented.

Geometric Approximation Model.

The main thrust of this approach is to perform most of the calculations prior to running WAM. This eliminates infeasible booster/DGZ combinations prior to model formulation which significantly reduces the number of decision variables in WAM.

The geometric approximation model capitalizes on the assumption that MIRV footprints can be successfully modeled using a geometric figure. Instead of calculating the complete set of feasible DGZ combinations for each missile system, which may be computationally unwieldy, a geometric figure is centered around each DGZ, and it is assumed that any laydown pattern within the figure constitutes an achievable sortie. As previously discussed, the ellipse is a logical choice as the geometric figure and is commonly used to model footprints (9:10). The specific dimensions of the ellipse depend on the range and missile flight profile. These dimensions can be set through manipulation of the parameters p and q, where p is the length of the semi-major axis and q is the length of the semi-minor axis. The length of the semi-major and semi-minor axis are determined

based on the missile type, configuration, and range. The ellipse is aligned such that the major axis is along the flight path from the launch point to the focal point DGZ.

This model requires calculation of a footprint ellipse for each DGZ/booster combination. However, it is assumed that launch vehicles grouped at the same launch site with similar weapon configurations generate the same footprints. Therefore, each DGZ needs to be considered only once per launch site/weapon configuration, which significantly reduces the number of ellipses which must be built (9:10). Since there are approximately 5000 targets, and estimating each is within range of three launch areas and seven submarine patrol areas, there are approximately 50,000 ellipses to be computed. However, since some closely located targets can be tied together into one DGZ, the actual number of DGZs may be somewhat smaller (7).

Once the footprint ellipses have been built, each DGZ can then be compared to each footprint. A DGZ is included in the footprint set of a centroid DGZ if the following inequality is true:

$$(\Delta D/p)^2 + (\Delta C/q)^2 < 1 \qquad (3-1)$$

Where:

p = half the down range stick length (the semi-major axis of the ellipse)

q = half the cross range stick length (the semi-minor axis of the ellipse)

ΔD = Down range displacement with respect to the centroid DGZ. This is

found using $\Delta D = Cos(LAz)\Delta Y + Sin(LAz) \Delta X$

ΔC = Cross range displacement with respect to the centroid DGZ. This is

found using $\Delta C = -Cos(LAz)\Delta X + Sin(LAz) \Delta Y$

LAz = Launch Azimuth, found using $LAz = ARCTAN(DGZ_{fX}/DGZ_{fY})$ where

DGZ_{fX} and DGZ_{fY} are the distance the centroid DGZ is displaced in

Longitude and Latitude, respectively, measured from the launch point

ΔX, ΔY = Distance displaced in Longitude and Latitude, respectively,

measured from the centroid DGZ
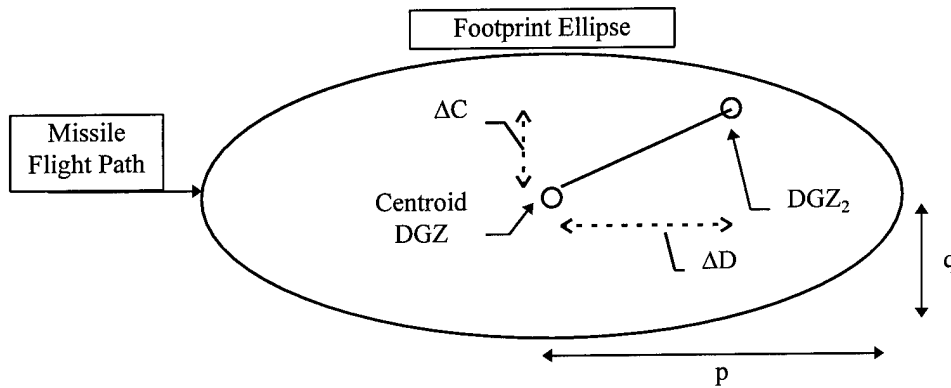
FIGURE 3-1. DGZ/Footprint Comparison

This requires approximately 5000 x 50,000 = 250 million comparisons. This is a

huge number, but the mathematics is relatively simple.

Since a launch area, missile type, and configuration define a booster, each

booster/DGZ combination has a corresponding ellipse. Include the binary variable

x_{ijk} in the model only if the footprint ellipse based on the ith booster, using the jth DGZ as the ellipse centroid, includes the kth DGZ.

Using preprocessing, only x_{ijk}'s that the geometric approximation (GA) model finds to be feasible are included in WAM.

GA Constraints. To develop the GA footprint constraints, two terms must first be defined:

a) Footprint set - the set of all DGZs that fall within a specific ellipse. Since an ellipse is defined for each launch site/DGZ combination, each booster has a corresponding footprint ellipse for each DGZ within range. Therefore, a footprint set can be defined by

$$S_{i,j} = \{k \text{ such that } x_{ijk} \text{ is included in WAM}\}$$

b) Strategy - a strategy is a means of attacking a target. It is defined by a number and type of weapon, and a DGZ against which the weapon is employed. A strategy is represented by the integer variable y_{ik}, where $y_{ik} = N$, if N weapons of type i are to attack DGZ k.

Once the infeasible x_{ijk}'s have been eliminated from WAM using the GA model, linear constraints can be used to ensure footprinting restrictions are met. These constraints must enforce the following goals:

a) Limit the maximum number of DGZs assigned to a booster to the number of RVs carried.

b) Limit the number of MIRVs that strike a particular DGZ to the maximum number called for by the attack strategy for that DGZ.

c) Ensure MIRVs from one booster strike DGZs from the same footprint set.

The following constraints enforce the above goals:

(DGZs per booster) $\qquad \sum_k x_{ijk} \leq R_i \quad \forall i \quad i, j, k \ \varepsilon \text{ GA restrictions}$

where R_i is the number of RVs carried on booster i.

(RVs per DGZ) $\qquad \sum_i \sum_j x_{ijk} - y_{ik} = 0 \quad \forall k$

In order to meet restriction c above, a variable must be defined to track whether or not a booster is using a particular footprint ellipse. Let the binary variable λ_{ij} take on a value of one if booster i targets a DGZ in footprint ellipse j, and a value of zero otherwise. Then the constraint for c above becomes

(one ellipse per booster) $\quad \sum_k x_{ijk} - R_i \lambda_{ij} = 0 \quad \forall i, j$

$$\sum_j \lambda_{ij} = 1 \quad \forall i$$

Energy Space Transformation

Since the geographic restrictions placed on a set of DGZs to be targeted by the same PBV stem from the limited energy available to the PBV, it seems logical that MIRV footprint constraints could be modeled using the energy required to displace the MIRVs. This is the fundamental principle behind the Energy Space Transformation model.

MIRV footprints are generally represented by geometric shapes drawn on a map of the earth's surface. This representation is referred to as geography space in this thesis. MIRV displacement in geography space has two components, cross

range displacement and down range displacement. If the energy per unit distance required to displace a MIRV were the same in cross range as in down range, then the total energy to displace a MIRV in geography space could easily be calculated using the Pythagorean Theorem. However, as stated earlier, it takes more PBV energy to displace a MIRV 1 kilometer in cross range than it does to displace the same MIRV 1 kilometer in down range (13:15). If the footprint constraints are modeled by summing the geographic distances from DGZ to DGZ, then the constraints will be nonlinear (4:10).

In order to form linear constraints, the footprint must be transformed into a framework whereby the distance between DGZs can be expressed in terms of PBV energy, as opposed to geographic distance. This involves mathematically manipulating the geographic coordinate expression for DGZs into an energy space coordinate expression, as illustrated by Figure 3-2.

Figure 3-2 shows the geometry required to develop the coordinate expression for the energy space model. Given the geographic coordinates for two DGZs and the azimuth of the missile flight path, it is desired to express the energy required to displace a MIRV. This will be represented by the coordinates (E_1, E_2), where E_1 and E_2 represent the energy needed for the down range and cross range components of the displacement, respectively. The azimuth is given as θ, which is the angle between the missile flight path and true north. ν is the angle between

true north and the line connecting the two DGZs. The geographic distance

between the two DGZs is d. In Figure 3-2 below, let DGZ 1 and DGZ 2 be given

in terms of latitude and longitude, (Lt_1, Ln_1), and (Lt_2, Ln_2), respectively. Then

the difference in latitude from DGZ 1 to DGZ 2 is $\Delta Y = Lt_2\text{-}Lt_1$.   Similarly, the

N θ

Missile
flight path

DGZ 2

E_2b

d

(E_1,E_2) = Energy Space
Coordinates

E_1a

ν γ

DGZ 1
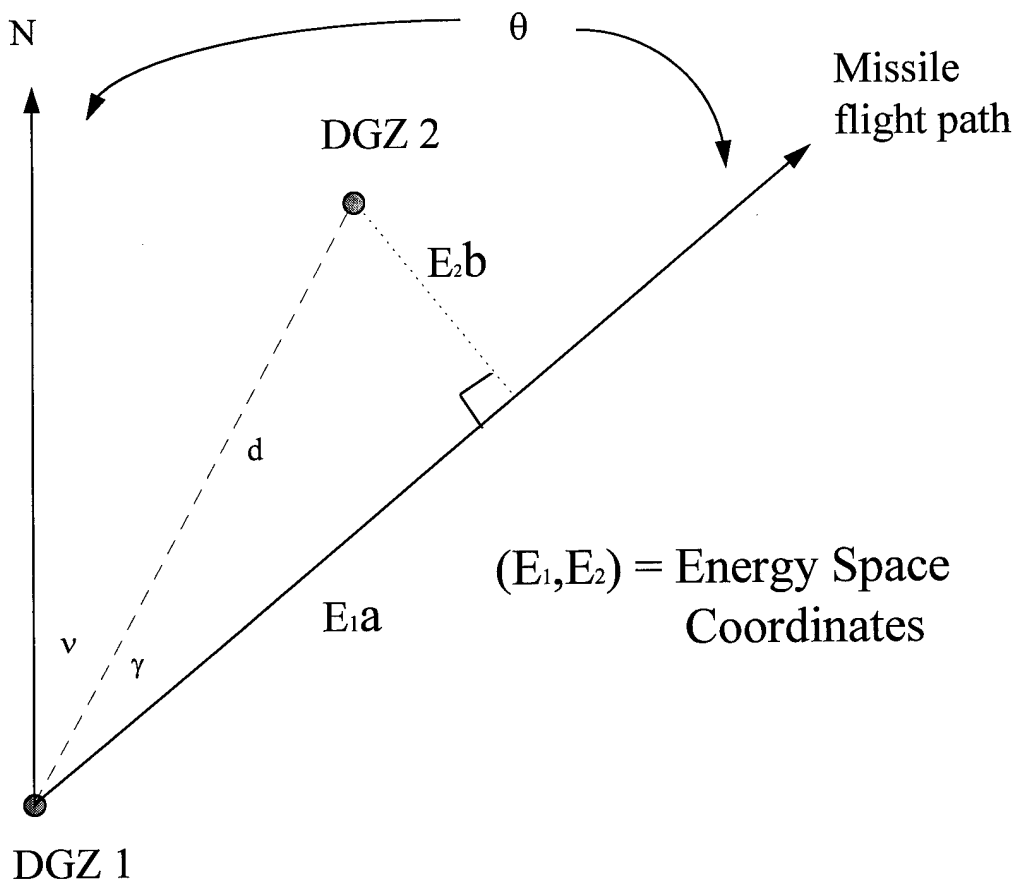
FIGURE 3-2. Energy Space Transformation Geometry.

difference in longitude is $\Delta X = Ln_2\text{-}Ln_1$. The distance, d, between the two

DGZ's can be found using the following equation (1:23-4).

$$d = 60 \text{ ARCCOS } [Sin(Lt_1)Sin(Lt_2) + Cos(Lt_1)Cos(Lt_2)Cos(\Delta X)] \qquad (3\text{-}2)$$

The key to converting geographic coordinates to energy space coordinates is to properly account for the difference in energy required for down range vs cross range MIRV displacement. Since the energy space model produces equal units of PBV energy per unit distance regardless of the direction of the displacement, the MIRV footprint in energy space is a circle, as opposed to the elliptical footprint in geography space. The circle is formed by scaling the down range and cross range distance using the parameters a and b, which are unique for each footprint. They can be thought of, respectively, as the semi-major axis and semi-minor axis of the geographic footprint ellipse. These two scaling parameters account for the difference in the energy required for down range and cross range displacement of the MIRV, such that a/b is the ratio of PBV energy required per unit cross range displacement to the energy required per unit down range displacement. Consider the following geographic footprint for a PBV with two MIRVs:
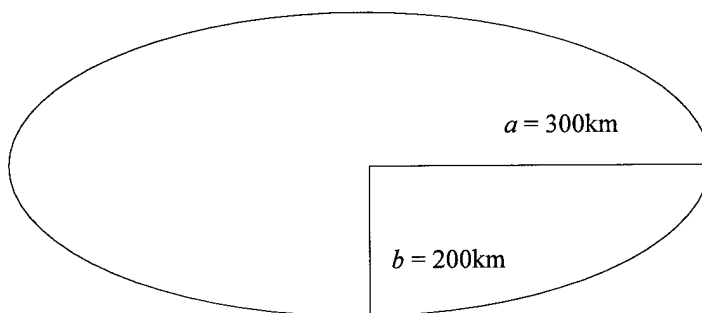
FIGURE 3-3. Geographic Footprint

Let the PBV corresponding to the above footprint have one unit of energy available. If the PBV uses all of its energy to perform a range extension on one MIRV, it can be seen from the footprint that this would equate to 300 km in down range. Or, the PBV could use all of its energy to displace one MIRV 200 km in cross range. Therefore, it takes one unit of energy per 300 km down range displacement and one unit of energy per 200 km cross range displacement. The energy space coordinates can now be calculated using E_1 = (down range displacement)/300, and E_2 = (cross range displacement)/200.

An expression for down range and cross range displacement must now be developed, since the DGZs are expressed in terms of latitude and longitude. Let ΔD and ΔC represent the down range and cross range displacement, respectively. From Figure 3-2, it can be seen that the displacement of DGZ 2 in cross range, ΔC, and down range, ΔD, can be expressed as

$$\Delta C = (\sin\gamma)d \qquad\qquad (3\text{-}3)$$

and

$$\Delta D = (\cos\gamma)d \qquad\qquad (3\text{-}4)$$

The angle γ can be expressed as $\theta\text{-}v$, so the above equations become

$$\Delta C = \sin(\theta\text{-}v)d$$

and

$$\Delta D = \cos(\theta\text{-}v)d$$

Using trigonometric relations (2:121)

$$\sin(\theta\text{-}v) = \sin\theta\cos v\text{-}\cos\theta\sin v$$

and

$$\cos(\theta-\nu) = \cos\theta\cos\nu + \sin\theta\sin\nu$$

So equations (3-3) and (3-4) can be written

$$\Delta C = (\sin\theta\cos\nu - \cos\theta\sin\nu)d$$

and

$$\Delta D = (\cos\theta\cos\nu + \sin\theta\sin\nu)d$$

Rearranging yields

$$\Delta C = \sin\theta(\cos\nu)d - \cos\theta(\sin\nu)d$$

and

$$\Delta D = \cos\theta(\cos\nu)d + \sin\theta(\sin\nu)d$$

From Figure 3-2, it can be seen that $(\cos\nu)d = \Delta Y$, the distance in the lattitudinal direction from DGZ 1 to DGZ 2, and $(\sin\nu)d = \Delta X$, the difference in longitudinal direction from DGZ 1 to DGZ 2. Therefore,

$$\Delta C = (\sin\theta)\Delta Y - (\cos\theta)\Delta X \qquad (3\text{-}5)$$

and

$$\Delta D = (\cos\theta)\Delta Y + (\sin\theta)\Delta X \qquad (3\text{-}6)$$

So in general, the equations for the energy space coordinates are

$$E_1 = [(\cos\theta)\Delta Y + (\sin\theta)\Delta X]/a \qquad (3\text{-}7)$$

and

$$E_2 = [(\sin\theta)\Delta Y - (\cos\theta)\Delta X]/b \qquad (3\text{-}8)$$

Once the energy space transformation is complete, the total PBV energy required to displace a MIRV from DGZ_i to DGZ_j, E_{ij}, can be calculated using $E_{ij} = (E_{1ij}^2 + E_{2ij}^2)^{1/2}$ where E_{1ij} and E_{2ij} are the down range and cross range energy, respectively, to displace a MIRV from DGZ i to DGZ j. Because a and b are ellipse parameters based on the maximum capability of the PBV, the values E_1 and E_2 can be thought of as the fraction of PBV energy required for the displacement. Let the term PBV Fractional Energy (PFE) be defined by the sum of all the E_{ij}'s for a PBV. If the PFE for a sortie is less than one, then the model considers that sortie feasible.

To implement the energy space model in a linear program, E_{ij} must be calculated for all values of i and j. This provides values for the PBV energy required to displace a MIRV from any DGZ to any other DGZ. However, because several launch areas may be in range of any DGZ, the energy distance from DGZ_i to DGZ_j varies depending on which footprint ellipse is used. So a third subscript, l, is needed to distinguish which booster generates the reference footprint. The constraint in the LP is then written as follows: (5:4)

$$\sum_j E_{lij} y_{lij} \leq 1 \qquad \forall\, l, i \qquad\qquad (3\text{-}9)$$

where:

E_{lij} is the energy distance from the ith DGZ to the jth DGZ, using the lth booster as the footprint reference.

y_{lij} is a binary variable indicating whether or not the jth DGZ is targeted by the lth booster with the ith DGZ as the missile focal point

32

Assumptions. The energy space transformation model approximates the actual energy used by accounting for the energy required to displace each MIRV from the missile focal point to its respective DGZ (3:4). In actuality, the PBV maneuvers for deployment of the MIRVs in some set sequence, from DGZ to DGZ (10:9). Therefore the actual energy used by a PBV is the sum of the energy needed to maneuver from one DGZ to the next in a specified order. In cases where there is a cluster of DGZs relatively close to each other, the model may be too restrictive. In the figure below, the energy space model accounts for the energy to displace MIRV 2 from DGZ 1 and MIRV 3 from DGZ 1. In actuality, once the PBV has maneuvered into position to deploy MIRV 2, a relatively small amount of energy would then be required to reposition for MIRV 3, as opposed to the
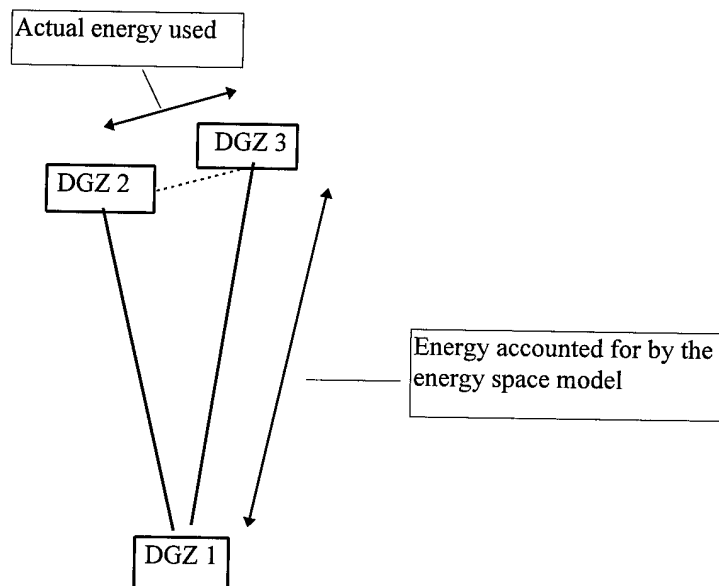
FIGURE 3-4. Actual PBV Energy Used to Displace a MIRV

larger amount of energy needed to displace MIRV 3 from DGZ 1 to DGZ 3.

There are two possible ways for the model to deal with this.

The first would be to sum the energy from DGZ to DGZ in order. The problem with this approach is that the model rapidly grows to an unmanageable size. To model the sequencing order in a linear programming format, the decision variables would have to have two additional subscripts, one to track the DGZ preceding the current DGZ, and one for the DGZ following the current DGZ (6). With approximately 5000 targets, there would be about 1.25×10^{11} decision variables (7).

The second way to deal with the approximation is to compensate by increasing the footprint ellipse size through parameter adjustment. This would be far easier to implement but would give less accurate results.

Another assumption of the energy space model is that the maneuvering energy remains constant throughout the missile flight. However, the energy required to displace a MIRV does not remain constant over time. As the PBV maneuvers, it gets lighter due to fuel expenditure and the release of RVs (10:14). This causes the energy required to displace the first RV 1 km in cross range to be greater than the energy required to displace the last RV 1 km in cross range. How significant this effect is depends on the weight of fuel expended, the number of RVs carried, and their weight relative to the PBV weight. The effect of this assumption is reduced somewhat by the fact that in the latter stages of the PBV maneuvering, there is less TOF remaining for MIRVs to gain separation.

Summary

This chapter developed the methodology to apply the geometric approximation and energy space transformation models. The methodology can be used to apply the models to test data to evaluate their performance. This will be accomplished in Chapter IV.

IV. Testing and Results

Introduction

In this chapter, the models are tested and refined as necessary to produce acceptable results. Integration of the models into WAM is also discussed.

Target Array

In order to build and test the footprinting models, a set of targets was required. This target array needed to be large enough to allow missile footprint ellipses of various sizes and alignments to be completely contained within the target area. In addition, the target array needed to be sufficiently dense to provide a significant number of challenging target combinations, yet be computationally manageable. Target area dimensions were selected to be 3000 nautical miles (nm) long by 2100 nm wide. Fifty DGZs were dispersed throughout the target grid by using a random number generator to produce the X and Y coordinates. The coordinates were rounded to the nearest 60 nm increment to simplify plotting and calculations. Six other DGZs were then strategically placed by hand to create clusters of DGZs. This was accomplished to better reproduce the type of target arrays encountered in real world planning. It should be stressed that in order to keep this document unclassified, the target array produced here was not generated using any real world target data. The DGZs were labeled from *A* to *BD*. The following is a visual representation of the target grid.
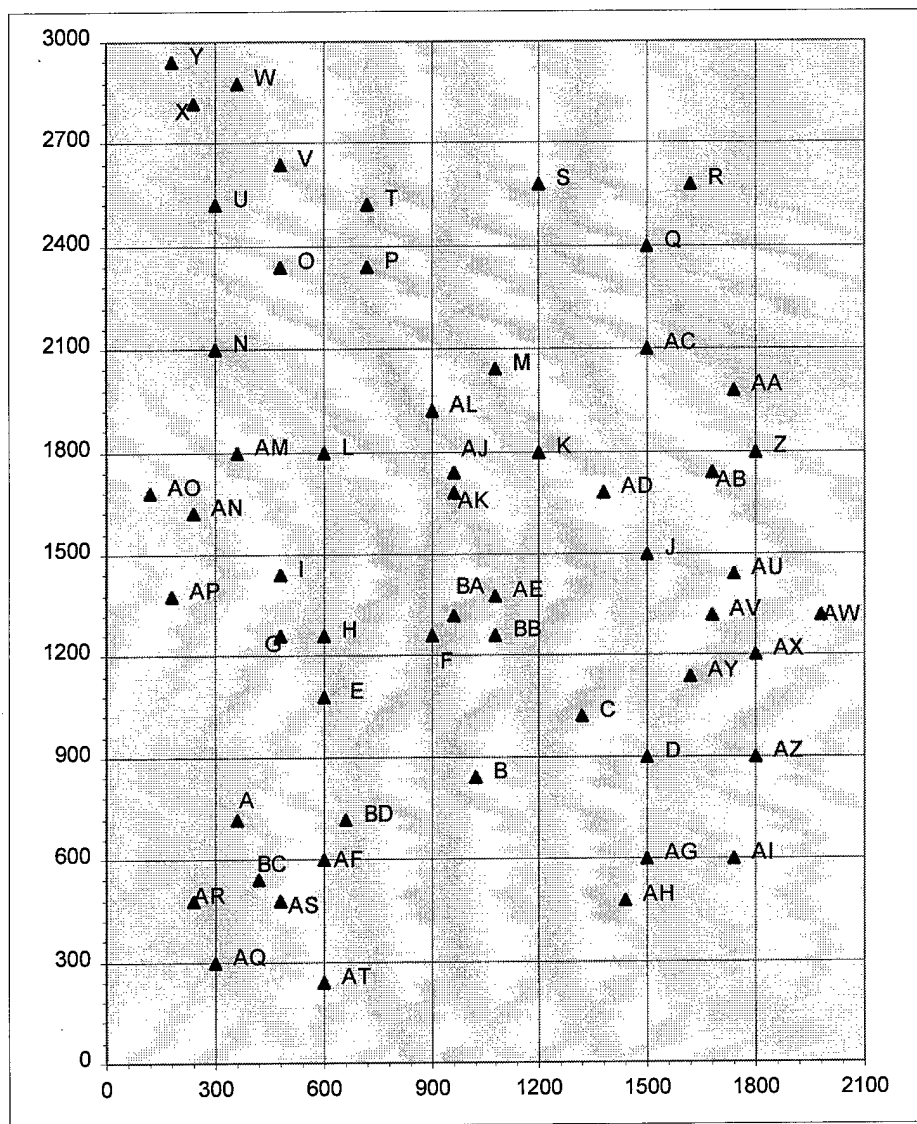
Figure 4-1. Target Area Grid (Units are in Nautical Miles)

Missile Simulation

In order to assess the proposed models, a high fidelity simulation is required to

provide data on the true capability of missile systems. The Microcomputer Missile

Performance Software System (MPS) was chosen to meet this requirement. MPS is

maintained by Kaman Sciences Corporation under the direction of the U. S. Air Force Studies and Analyses Agency (12:iii). It provides a detailed model of every aspect of a ballistic missile's flight. This gives an accurate assessment of the performance of missile systems used in this research. The user defines booster, Post Boost Vehicle (PBV), and Reentry Vehicle (RV) subsystems by providing a series of parameter inputs. A missile system is then defined by a combination of one of each of the above subsystems. MPS can provide a variety of outputs including maximum booster range, PBV down range and cross range stick lengths, and sortie feasibility reports which include the percentage of PBV fuel remaining at each RV deployment.

Missile Systems

The missile systems used in this research are fictitious. In order to provide a more thorough analysis of the models, two different missile systems were used. These missile systems were designed with capabilities that provide a rigorous test of the methodology and models presented.

The first missile system chosen for use is the US-3RV system contained in the MPS sample data file. The system carries three RVs, each weighing 1167 pounds. The RVs are carried on a pusher, nose forward type PBV with a dry weight of 2435 pounds and a usable fuel weight of 1394 pounds. A three stage booster is used to launch the PBV assembly. The maximum booster range of the US-3RV system without using PBV fuel for PBV range extension is 4840 nm.

The second missile system is called the US-4RV system. This missile uses the same booster and RVs as the US-3RV system. The PBV is modified to carry a fourth

RV. Because of the added RV, the PBV footprint would be too small in relation to the

DGZ density to provide good test data. Therefore the PBV parameters were modified to

make the footprint size more useful. Table 4-1 gives the PBV parameters that were

changed. Due to the added weight of the fourth RV and the additional PBV fuel, the

maximum range of the US-4RV system is reduced to 3854 nm.

Table 4-1. PBV Parameters.

Parameter	US-3RV	US-4RV
Usable Fuel Weight (lb.)	1394	1800
Axial Engine Thrust (lb.)	165.6	200
Specific Impulse (sec)	306.6	320

Launch Areas

In order to reduce the possibility that anomalies in the target array may bias the

overall results, and to increase the randomness of the model tests, two widely separated

launch areas were used. Each launch area represents a missile field. Since missile

systems fired from the different launch areas approach the target grid from different

angles, the same set of DGZs can provide a completely different footprinting problem.

Thus, using two widely separated launch sites provides results similar to that of using two

different target arrays. The only exception is that the DGZ density is the same regardless

of which launch site is used. The two launch sites, designated LS1 and LS2, are situated

with respect to the target area as shown in Figure 4-2. LS1 is used for the US-3RV

system. LS2 operates the US-4RV system. The ranges from the respective launch sites to the target area were selected to provide a usable footprint size with respect to the DGZs, and also to ensure that the majority of the target area would be in range of the respective missile system.
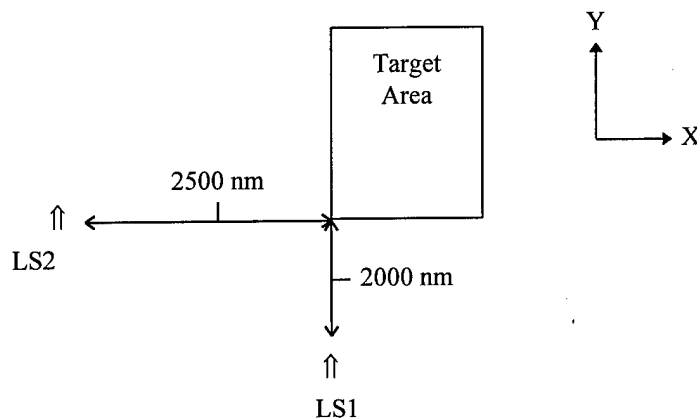
Figure 4-2. Launch Site Orientation.

Assumptions

Several assumptions are made in the application of the MPS simulation to isolate the factors effecting the model results. First, all missile sorties are flown assuming a perfectly spherical earth. Although the effect of this assumption on the model results is small, accounting for the oblateness of the earth would cause various changes in the results depending on the locations of the launch site/target area on the earth and the direction in which the missile is fired. It is desired to analyze sortie results only with respect to changes in the models or changes in missile system/DGZ combinations. Excluding the spherical earth assumption would produce variations in the simulation results for reasons other than model changes or missile system/DGZ combinations.

A non-rotating earth is also assumed. If this assumption is not made, the distance a missile has to travel to complete a sortie would be affected by its launch azimuth. A particular arrangement of DGZs may be feasible from LS2 but not from LS1 simply because the DGZs are rotating away from LS1 throughout the missile flight. Such an effect would cause undesirable perturbations to the model results.

For sorties that do not use a maximum range trajectory, a maximum time of flight trajectory (TOF-I) is used. This is based on the assumption discussed in Chapter II regarding over-lofted vs under-lofted trajectories. Also, each missile sortie simulated using MPS uses the minimum energy reentry angle.

MPS is programmed to require sorties to maintain a minimum interobject spacing of 90,000 ft (approximately 15 nm). This restriction is also in effect for the sorties used to build stick length curves. This ensures the models are sensitive to interobject spacing requirements.

Stick Length Curves

Several sorties were simulated using various ranges-to-first-target for both the US-3RV and US-4RV systems. All of the above assumptions were incorporated into the MPS input data. MPS output includes both the down range and cross range stick lengths. It should be remembered that these values are mutually exclusive. If a sortie is flown to achieve its maximum down range stick length, then no energy is available for cross range displacement and visa versa. The following graphs depict the stick length data over the ranges that may be encountered in this research.

Table 4-2. Stick Length Data for US-3RV System

Range (nm)	Down Range Stick (nm)	Cross Range Stick (nm)
2000	756	286
2500	988	331
2750	1128	347
3000	1265	363
3250	1418	379
3500	1617	388
3750	1809	402
4000	2015	412
4250	2288	417
4500	2543	422
4750	2802	428
4840	2940	429
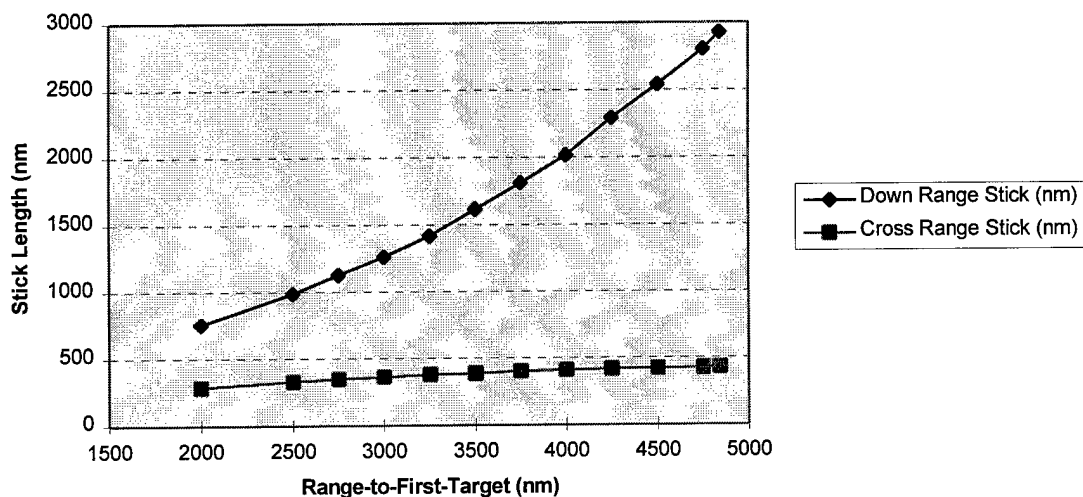
Figure 4-3. Stick Lengths for US-3RV System

Table 4-3. Stick Length Data for US-4RV System

Range (nm)	Down Range Stick (nm)	Cross Range Stick (nm)
2000	847	314
2500	1141	364
2750	1310	387
3000	1484	410
3250	1678	429
3500	1921	441
3750	2161	456
3854	2274	461
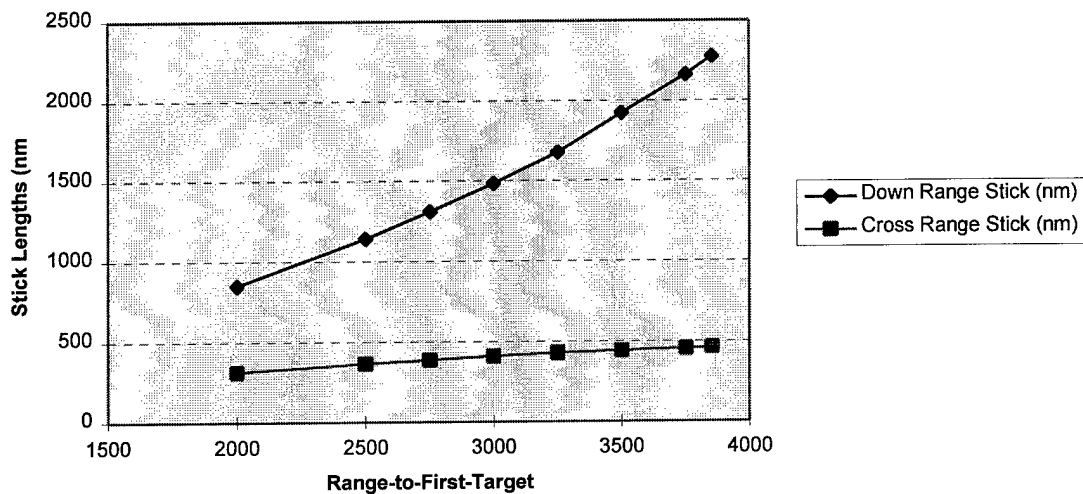
Figure 4-4. Stick Lengths for US-4RV System

To set the scaling parameters and ellipse dimensions, the models require stick length values for a given range-to-first-target. Therefore a mathematical model of the stick length curves is required. An inspection of the plots shows that each stick length

can be reasonably approximated using linear regression. The linear regression equations

for each stick length were computed and are listed in Table 4-4. In the equations, R

represents the range to the first target. If footprint ellipses for each system are

constructed based on the stick length dimensions, then the ratio of the major axis to the

minor axis for the ellipses increases from approximately 2.5 to 5, as range increases.

Table 4-4. Linear Regression Equations for Stick Length

	Down Range	Cross Range
US-3RV	0.63R-582	0.063R+160
US-4RV	0.75R-715	0.081R+152

Preliminary Computations for Model Implementation

The Geometric Approximation (GA) and Energy Space Transformation (EST)

models were set up using an Excel spreadsheet. The distances in the X and Y directions,

ΔY and ΔX, from each LS to each DGZ were computed. These values were then used to

calculate the range-to-first-target for each DGZ using $R = (\Delta Y^2 + \Delta X^2)^{1/2}$. Note that

planar geometry calculations were used here to set up the test sorties. This was done to

make it easier to visualize the footprints on the two dimensional target grid. This has no

bearing on the validity of the test since the DGZs could have been plotted in a spherical

coordinate system in such a way as to produce the exact same parameters for each sortie.

The launch azimuths for each sortie were also required for subsequent calculations in the model. Here, launch azimuth is defined as the angle between the line segment connecting the launch site with the first DGZ and the line segment connecting the launch site with the bottom left corner of the target area (refer to Figure 4-2). For LS1, for example, a launch azimuth of zero degrees would define a trajectory heading in the Y direction, while a launch azimuth of zero degrees from LS2 would define a trajectory heading in the X direction. This convention was used to simplify the computer coding and has no bearing on the model results.

Geometric Approximation Testing

Footprint ellipse dimensions were calculated for each launch site/DGZ combination. Given one of the 56 DGZs, let p be the length of the major axis of the ellipse and q be the length of the minor axis. Then p and q are calculated using the linear approximations for down range and cross range stick length, respectively. For this calculation the range to the centroid DGZ was used for R in the linear approximation equations. This resulted in a total of 112 footprint ellipses, each with a DGZ at the centroid. Equations (3-7) and (3-8) in Chapter III were then used to compare all 56 DGZs to all 112 ellipses. The results were used to build footprint sets. A footprint set is defined as the set of DGZs contained within the footprint ellipse for a specific centroid DGZ. Each DGZ has a footprint set for each launch site, since each DGZ is the centroid of an ellipse based on a particular launch site.

Initial comparisons between GA and MPS results immediately revealed a problem with the GA model. The problem was due to an inconsistency in sequencing

45

requirements. When using the GA model, the centroid DGZ is required to be the focal

point DGZ since the range used to size the ellipse is based on this DGZ. (Recall that

"centroid DGZ" defines the DGZ at the centroid of the ellipse, while "focal point DGZ"

refers to the missile aimpoint, which is the first DGZ to be struck in sequence.) However,

the minimum energy sequence for a PBV almost always begins with a peripheral DGZ.

Striking the centroid DGZ first in the sequence often creates an infeasible sortie even

though sequences starting with outer DGZs would have worked. Figure 4-5 illustrates this

concept. In case 1, the DGZs a, b, and c, can be feasibly struck in that sequence

according to MPS. But if a is used in the GA model as the focal point DGZ, then the

model requires it to also be the centroid DGZ. Thus, the footprint ellipse is centered

around a, and does not include c. So the GA model will falsely reject the sortie. In case

2, GA uses DGZ b as the centroid, so the ellipse now encloses all three DGZs, and the

ellipse dimensions are now based on the range to b. Since the ellipse centered at b

encloses all DGZs, the GA model would classify the sortie as feasible. However, the

sortie striking DGZ b first in the sequence is found by MPS to be infeasible because of

the energy required to maneuver from the center of the footprint to an outer edge, and

then backtrack all the way to the other end of the ellipse. The PBV lacks sufficient

energy to strike the DGZs in this sequence. To be successful, the model

must somehow ensure that the focal point DGZ is one that is located on the fringes of the

set of DGZs to be footprinted. This prevents the PBV from having to waste energy

backtracking through the footprint, which is inevitable when the first DGZ is centrally

located. But the ellipse must still be centrally located in order to enclose the DGZs in a

feasible footprint.

A modified version of the GA model was developed to solve this problem. In the modified model, the length of the ellipse is doubled, but feasible footprints are restricted to those that have all ΔD values positive with respect to the focal point DGZ. In other words, all DGZs must be down range of the focal point DGZ. This, in effect, uses half of an ellipse to form the footprint. Doubling the ellipse length ensures feasible DGZs are still enclosed by the footprint. Case 3 in Figure 4-5 illustrates the modified model. In this case, a is the centroid DGZ for constructing the GA ellipse, and the focal point DGZ for both models. Both GA and MPS score the sortie [a-b-c] as feasible. After the model was modified to incorporate the above changes, a new set of 112 ellipses was computed and the DGZ comparisons were made. From these comparisons, a footprint set was constructed for each footprint ellipse. A listing of these sets is included in Appendix A.

Test Sortie Selection. To test every possible sortie would not be possible within the scope of this research due to limitations of the MPS software. The US-4RV system alone has $\binom{56}{4}$, or 367,290 possible DGZ combinations. But since the stick lengths for the missile systems, and therefore the footprint ellipses, are fairly small with

Case 1.	Case 2.	Case 3.
MPS - Yes	GA - Yes	GA - Yes
GA - No	MPS - No	MPS - Yes

c. Δ   c. Δ   c. Δ

b. Δ   b. Δ   b. Δ

a. Δ   a. Δ   a. Δ
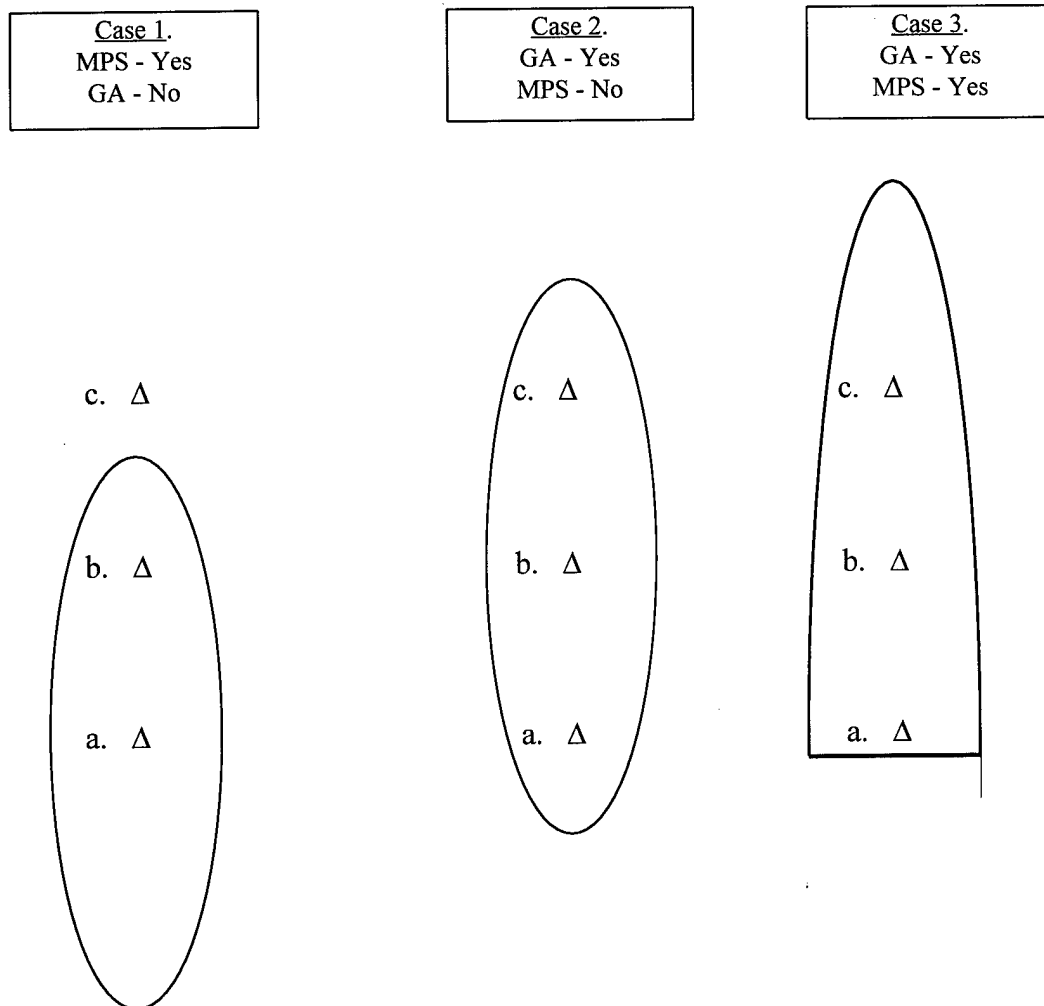
Figure 4-5. GA Cases.

respect to the size of the target grid, the vast majority of the possible DGZ combinations

would constitute infeasible sorties. Therefore, a total enumeration of all the possible

sorties would not prove useful. Both the geometric approximation model and the energy

space transformation model can easily identify sorties that are grossly infeasible. So, to

provide a meaningful test of the models, it is necessary to select borderline sorties that

require either slightly more or slightly less than the maximum capability of the PBV. For a valid and challenging test, the test sorties should be split evenly between feasible and infeasible sorties. To demonstrate this, consider a test where most of the test sorties are infeasible sorties. The model could use an ellipse size of zero, yet within the confines of the test be correct a majority of the time. The same is true of a test where the majority of the test sorties are feasible. A model with an infinite ellipse size could correctly classify the test sorties the majority of the time, even though such a model is obviously useless. By testing the models on even numbers of feasible and infeasible sorties, a true measure of the effectiveness of the models is achieved.

The GA model was used as a basis for selecting the test sorties. Using the footprint sets produced by GA, eighty test sorties were generated - forty for the US-3RV system and forty for the US-4RV system. Twenty of the sorties for each system were classified as feasible by the GA model, and twenty were classified as infeasible. To provide the most challenging test possible, the GA-feasible sorties were chosen by first selecting a footprint set at random. The footprint set was then studied to find one of the most challenging DGZ combinations that was still considered feasible by the GA model. For example, sorties where one or more of the DGZs fall close to the ellipse perimeter or where the DGZs are on opposite sides of the ellipse provide the greatest challenge to the PBV. If a sortie classified as feasible by GA was selected where all the DGZs were in close proximity and in a straight line, the PBV would have no difficulty in completing the sortie. If only sorties similar to these were selected for the test, the results would be

biased in favor of the models. Examples of each of these cases are presented in Figure 4-6.
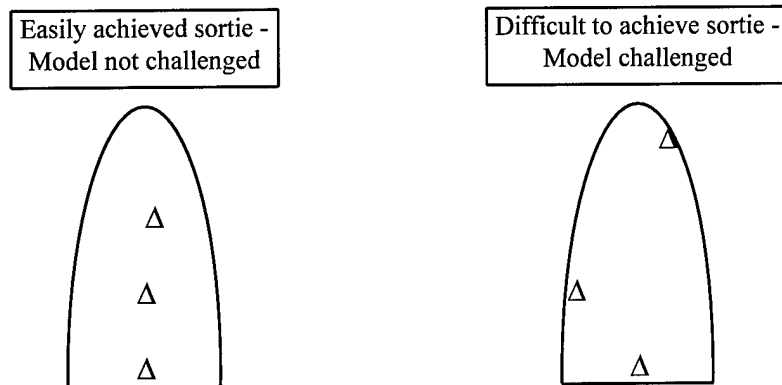
Figure 4-6. Test Sortie Selection Cases.

The same principle was used to select the GA-infeasible test sorties. Footprint sets were randomly selected, and then a sortie was constructed using an easily achievable combination of DGZs. Then one DGZ from the sortie was exchanged for a DGZ located just outside of the footprint ellipse. This technique provided a set of sorties that were classified as infeasible by GA, yet were very close to being classified as feasible. If the models were to make errors, it is most likely that they would occur on these borderline sorties. Therefore, if the models perform well on this worst case group of sorties, they should have no problems handling the full range of target data. The following table lists the eighty test sorties. The column labeled "Geo Apx" indicates whether or not the geometric approximation model classifies the sortie as feasible.

Table 4-5. Test Sorties

Sortie #	Launch Site	Focal pt DGZ	DGZ 2	DGZ 3	Geo Apx	Sortie #	Launch Site	Focal pt DGZ	DGZ 2	DGZ 3	DGZ 4	Geo Apx
1	1	A	G	I	Y	41	2	A	AF	B	C	Y
2	1	B	AE	AD	Y	42	2	A	BD	B	C	Y
3	1	E	G	H	Y	43	2	B	C	D	AZ	Y
4	1	G	I	L	Y	44	2	AS	AF	AG	AI	Y
5	1	G	I	P	Y	45	2	C	AY	AV	AX	Y
6	1	H	I	P	Y	46	2	BC	AS	AF	BD	Y
7	1	I	AM	T	Y	47	2	E	F	BB	J	Y
8	1	L	T	P	Y	48	2	E	F	BB	AU	Y
9	1	N	O	Y	Y	49	2	F	BA	BB	J	Y
10	1	O	U	V	Y	50	2	G	H	AE	AB	Y
11	1	AB	Z	AA	Y	51	2	H	F	BA	BB	Y
12	1	AC	Q	R	Y	52	2	I	AK	AJ	AA	Y
13	1	AD	Q	R	Y	53	2	BA	AE	J	Z	Y
14	1	AE	K	Q	Y	54	2	AR	AQ	AS	AF	Y
15	1	AT	AF	BD	Y	55	2	AE	J	AB	Z	Y
16	1	BB	BA	Q	Y	56	2	AF	BD	B	AG	Y
17	1	BA	AE	M	Y	57	2	AF	BD	B	AZ	Y
18	1	BC	G	H	Y	58	2	AJ	AL	M	AC	Y
19	1	BC	A	H	Y	59	2	AR	AS	BC	BD	Y
20	1	BD	F	AJ	Y	60	2	BA	AE	J	AU	Y
21	1	BD	F	BA	N	61	2	A	AF	B	AY	N
22	1	A	G	H	N	62	2	A	BC	AS	AF	N
23	1	A	G	AK	N	63	2	BB	AE	J	AW	N
24	1	F	K	AC	N	64	2	E	BB	J	AB	N
25	1	H	I	AK	N	65	2	E	F	BB	AW	N
26	1	I	AK	L	N	66	2	F	BA	BB	Z	N
27	1	L	O	P	N	67	2	L	AK	AJ	K	N
28	1	AD	AC	AA	N	68	2	AE	J	AU	AW	N
29	1	AE	K	AC	N	69	2	AF	B	C	D	N
30	1	AF	BD	F	N	70	2	BB	AE	AY	AV	N
31	1	AG	D	AY	N	71	2	BA	AE	J	AV	N
32	1	AK	L	AL	N	72	2	BA	AE	J	AX	N
33	1	AM	U	W	N	73	2	AJ	K	AC	Q	N
34	1	AO	U	X	N	74	2	AJ	K	AD	AC	N
35	1	AP	AN	Y	N	75	2	AK	AJ	K	AA	N
36	1	AQ	AS	BC	N	76	2	AK	AJ	K	AD	N
37	1	AS	BC	A	N	77	2	F	AE	AD	AB	N
38	1	AS	BC	G	N	78	2	F	BB	AE	AU	N
39	1	AT	AS	AF	N	79	2	B	C	AY	AU	N
40	1	BC	G	I	N	80	2	B	C	AY	AW	N

DGZ Sequencing

DGZ sequencing is a critical part of any footprint study. As discussed in Chapter II, a set of DGZs may form a feasible sortie in one sequence, but not in another. Therefore, when making comparisons between model results and MPS results, it is necessary to test all possible DGZ sequences using MPS before declaring a sortie infeasible. The exception to this rule is the first DGZ. Since the time of flight of a missile, and therefore the ellipse dimensions, are based on the range to the focal point DGZ, the model should use the focal point DGZ as the centroid DGZ. In other words, the DGZ at the center of the footprint ellipse should be struck first by the missile to ensure the ellipse dimensions are based on the correct missile range. To place another DGZ first in the sequence may cause MPS to give a false feasible result due to a longer range-to-first-target than is actually being used. Therefore, when sorties were tested on MPS, the first DGZ, or focal point DGZ, was fixed as the centroid DGZ, and then every possible sequence of the subsequent DGZs was tested.

Error Types

In order to better assess the effectiveness of the models, it is necessary to distinguish between the two possible types of model errors. In this research, a type I error is defined as an error where the model classifies a sortie as feasible that is found by MPS to be infeasible. A type II error occurs when a model classifies a sortie as infeasible when MPS finds the sortie feasible.

Initial GA Results

Each of the eighty test sorties was simulated using MPS. Table 4-6 lists the

Table 4-6. Initial GA Results.

Sortie #	Geo Apx	MPS / %REM	Sortie #	Geo Apx	MPS / %REM
1	Y	Y/22	41	Y	N
2	Y	N	42	Y	Y/11
3	Y	Y/23	43	Y	Y/10
4	Y	Y/47	44	Y	N
5	Y	Y/18	45	Y	Y/18
6	Y	N	46	Y	Y/29
7	Y	N	47	Y	Y/15
8	Y	Y/37	48	Y	Y/10
9	Y	Y/0.09	49	Y	Y/32
10	Y	Y/10	50	Y	Y/2
11	Y	Y/43	51	Y	Y/28
12	Y	Y/48	52	Y	Y/1
13	Y	Y/24	53	Y	Y/30
14	Y	Y/21	54	Y	N
15	Y	Y/26	55	Y	Y/23
16	Y	N	56	Y	N
17	Y	Y/12	57	Y	N
18	Y	N	58	Y	Y/2
19	Y	Y/2	59	Y	Y/21
20	Y	N	60	Y	Y/37
21	N	Y/20	61	N	N
22	N	Y/27	62	N	Y/5
23	N	N	63	N	N
24	N	N	64	N	N
25	N	N	65	N	N
26	N	N	66	N	Y/9
27	N	N	67	N	Y/18
28	N	Y/12	68	N	Y/9
29	N	Y/19	69	N	N
30	N	Y/23	70	N	N
31	N	Y/26	71	N	Y/23
32	N	N	72	N	Y/3
33	N	Y/24	73	N	N
34	N	Y/8	74	N	N
35	N	N	75	N	Y/28
36	N	Y/20	76	N	Y/24
37	N	Y/43	77	N	Y/20
38	N	Y/6	78	N	Y/12
39	N	Y/5	79	N	Y/3
40	N	Y/2	80	N	Y/21

results provided by the GA model and by MPS. For feasible sorties, MPS provides the percentage of PBV fuel remaining after the last MIRV is deployed. This value gives a useful measure of how easy the sortie was for the PBV to complete, and is included in the table in the *MPS/% REM* column. For example, the PBV was able to successfully complete sortie 40 with 2% of its fuel remaining.

The results in Table 4-6 show that GA was correct in classifying 55% of the sorties. Of the 36 errors, 11 were type I and 25 were type II. Nineteen of the errors occurred on US-3RV sorties, compared to seventeen for the US-4RV system.

Problems with GA Model. A close examination of the sorties that the model failed to properly classify revealed some weaknesses in the model. When the model made type I errors, they were frequently caused by DGZ combinations that forced the PBV to retrace its steps in the cross range direction. Consider sortie 54 as an example.
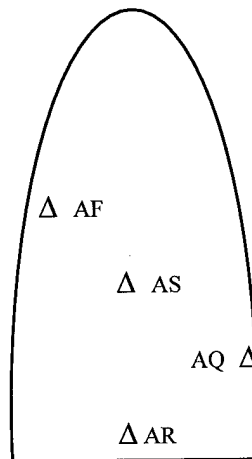
Figure 4-7. Sortie 54

Figure 4-7 depicts sortie 54 with the GA footprint ellipse. Recall that the width of the ellipse is based on the cross range stick length of the missile system and on the range to DGZ *AR*, which is 2781 nm. Since the width of the ellipse is equal to the cross range stick length, this means that it takes all of the PBV energy to evenly space MIRVs from one side of the ellipse to the other. The GA model, in its current form, requires the first DGZ to be centered in the ellipse. This leaves open the possibility of selecting DGZ combinations that force the PBV to maneuver toward one side of the ellipse, as it does in this sortie to strike *AQ*, and then maneuver back to the other side to strike other DGZs. The total sum of the cross range distance covered rapidly exceeds the cross range stick length distance, and exhausts the PBVs energy before the sortie is complete. For sortie 54, any DGZ sequence starting with *AR* will require the PBV to maneuver in the cross range direction about 1.5 times the cross range stick length. This is similar to the problem experienced in the down range axis that was eliminated by using the half ellipse to fix the first DGZ on the leading edge of the footprint. Although this did reduced zigzagging in the down range direction, the same solution cannot be applied in the cross and down range directions at the same time. However, the stick length curves show that in this sortie the ellipse ratio is almost four to one. This corresponds to a requirement of almost four times the PBV energy to maneuver in cross range an equal distance in down range. So if the DGZ sequence were not required to hinge on DGZ *AR*, the PBV may actually be able to complete the sortie and the GA model's classification of feasible would be correct. With this in mind, the sortie was retried on MPS using the sequence *AF, AS, AR,*

AQ. The PBV successfully completed the mission with 2% fuel remaining. Therefore, it can be concluded that depending on how the DGZs are positioned, some sorties need to sequence across the footprint in the cross range direction and some sorties need to sequence in the down range direction. In order to successfully model both types of sorties, GA must afford more flexibility for sequencing.

The second weakness found in the model reinforces the above conclusion. A close examination of sorties that triggered type II errors revealed a common problem. Consider sortie 37, depicted below.
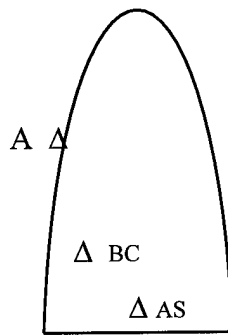
Figure 4-8. Sortie 37

With DGZ *AS* as the ellipse centroid, the footprint ellipse does not enclose *A,* causing GA to reject the sortie. But MPS, using *AS* as the focal point, found the sortie to be feasible with 43% of the PBV fuel remaining. Although the DGZs are separated primarily in cross range, the total cross range displacement from *AS* to *A* is less than the width of the ellipse. This accounts for the ease in which the PBV completed the sortie. However, by restricting the focal point DGZ to be the centroid DGZ, the GA model in its current form

forces the ellipse to be centered around *AS*. This makes it impossible for the ellipse to enclose *A*, even though the sortie is actually feasible. Several other sorties triggered type II errors due to similar circumstances. A simple solution would be to increase the width of the ellipses beyond the cross range stick length to compensate for this problem, but that would worsen the problems causing the type I errors. If GA could use *BC* as the centroid of a full ellipse, then the DGZs would be enclosed, even with the current dimensions. Therefore, as stated above, the GA model needs to have more flexibility with regard to sequencing.

Unhinged Geometric Approximation Model

To address the problems with the geometric approximation model, two modifications were made. First, the requirement for the focal point DGZ to also be the centroid DGZ was lifted. Second, the full ellipse was restored with dimensions equal to the stick lengths. This allowed any DGZ in a sortie to be tried as the centroid DGZ. But unlike the previous version of the model, any other DGZ in the sortie can be used as the focal point DGZ by the actual missile. Therefore, any DGZ in the test sorties can be used as the focal point for determining the feasibility of the sortie with MPS. Thus, the model focuses on identifying sets of DGZs that fall within the ellipse without requiring them to hinge upon any particular focal point DGZ. This enabled the model to more strongly reflect the proximity of the DGZs, as opposed to their pattern of arrangement. Interviews with current users of AEM (future users of WAM) revealed that there is no need for the model to specify a feasible DGZ sequence. The purpose of the model is to identify sets of DGZs that can be successfully footprinted. The actual focal point selection and

sequencing is left to the operational planner (10). The disadvantage of this modification is that, as previously discussed, the ellipse dimensions may be based on a centroid DGZ that is not the actual focal point DGZ used by the missile to successfully accomplish the sortie. Thus the ellipse dimensions may differ slightly from the appropriate dimensions for the range to the ellipse centroid. But even with this disadvantage, the tradeoff to improve the flexibility of the ellipse placement should increase the overall accuracy of the model. The new version of the GA model is referred to as the unhinged version of the geometric approximation model (GAU).

GAU Testing Results. The eighty test sorties were used to test the new GAU model. The results showed a dramatic improvement over the original model. Table 4-7 lists the GAU results for the eighty test sorties under the column labeled "Unhinged", along with the original GA results and the MPS results. Sorties where GAU errors exist are highlighted in bold. The GAU model classified 77.5% of the test sorties correctly. Note that the two example sorties, sortie 54 and sortie 37, were both correctly classified by the GAU model. Sortie 54 was still classified as feasible by GAU, but now MPS can use a more efficient focal point to show that the DGZ set [*AR-AS-AF-AQ*] actually can be successfully footprinted. The problem with sortie 37 was also fixed, since the ellipse centered around DGZ *BC* creates a footprint set including *A* and *AS*.

Table 4-7. Unhinged Geometric Approximation Results

Sortie #	Geo Apx	Unhinged	MPS / %REM	Sortie #	GEO APX	Unhinged	MPS / %REM
1	Y	Y	Y/22	41	Y	Y	N
2	Y	N	N	42	Y	Y	Y/11
3	Y	Y	Y/23	43	Y	Y	Y/10
4	Y	Y	Y/47	44	Y	Y	N
5	Y	Y	Y/18	45	Y	Y	Y/18
6	Y	Y	N	46	Y	Y	Y/29
7	Y	N	N	47	Y	Y	Y/15
8	Y	Y	Y/37	48	Y	Y	Y/10
9	Y	Y	Y/.09	49	Y	Y	Y/32
10	Y	Y	Y/10	50	Y	Y	Y/2
11	Y	Y	Y/43	51	Y	Y	Y/28
12	Y	Y	Y/48	52	Y	Y	Y/1
13	Y	Y	Y/24	53	Y	Y	Y/30
14	Y	Y	Y/21	54	Y	Y	Y/2
15	Y	Y	Y/26	55	Y	Y	Y/23
16	Y	Y	N	56	Y	N	N
17	Y	N	Y/12	57	Y	Y	N
18	Y	Y	N	58	Y	Y	Y/2
19	Y	N	Y/2	59	Y	Y	Y/21
20	Y	Y	N	60	Y	Y	Y/37
21	N	Y	Y/20	61	N	Y	N
22	N	Y	Y/27	62	N	Y	Y/5
23	N	N	N	63	N	Y	N
24	N	N	N	64	N	Y	N
25	N	N	N	65	N	Y	N
26	N	N	N	66	N	Y	Y/9
27	N	N	N	67	N	Y	Y/18
28	N	N	Y/12	68	N	Y	Y/9
29	N	N	Y/19	69	N	Y	N
30	N	N	Y/23	70	N	N	N
31	N	Y	Y/26	71	N	Y	Y/23
32	N	N	N	72	N	Y	Y/3
33	N	Y	Y/24	73	N	N	N
34	N	Y	Y/8	74	N	Y	N
35	N	N	N	75	N	Y	Y/28
36	N	Y	Y/20	76	N	Y	Y/24
37	N	Y	Y/43	77	N	Y	Y/20
38	N	Y	Y/6	78	N	Y	Y/12
39	N	Y	Y/5	79	N	Y	Y/3
40	N	Y	Y/2	80	N	Y	Y/21

59

Table 4-8 breaks down the total errors by type and missile system.

Table 4-8. GAU Error Breakdown

	TYPE I	TYPE II
US-3RV	4	5
US-4RV	9	0

The fact that there are significantly more type I errors than type II errors indicates that the ellipse dimensions may be too large. This is especially true in the case of the US-4RV system, where all nine errors were type I. It is reasonable to expect the ellipse sizes would have been too large for the unhinged model, since the focal points are no longer restricted to the DGZs closest to the launch site. The occasional use of more distant DGZs as focal points causes the missile ranges to be longer on the average, creating larger footprint ellipses. To compensate, the ellipses' dimensions can be reduced slightly. Adjusting the ellipse dimensions changes the proportion of errors that are type I and type II. When the ellipse dimensions are such that the model produces a fairly even split between type I and type II errors, then the dimensions are close to optimum.

To illustrate this, consider the sources of error for the models. These sources can be classified in two basic groups. The first can be referred to as model error, and includes all error induced by the model assumptions and approximations. Examples of model

errors are errors caused by the linear regression approximation of the stick lengths, and errors induced by the assumption that the energy required to maneuver the PBV remains constant over time even though the PBV gets lighter due to fuel expenditure and RV release. Model errors are random and are not biased toward causing larger numbers of either type I or type II errors. The second group of error sources includes errors induced by improper ellipse size. Changing the ellipse size changes both the number and the type of errors. If the ellipse size is far too large or far too small, there are a significant number of errors as a result. The error caused by improper ellipse size is biased in that it produces more of one type of error than the other. If an ellipse is excessively large, then there are more false acceptances (type I errors) than false rejections (type II errors). Reducing the ellipse's dimensions reduces the total number of errors by eliminating more type I errors than the number of type II errors that are created. If the ellipse dimensions are reduced in small increments, a point would eventually be reached where any further reduction would not cause a reduction in the total number of errors. This point corresponds to the optimal ellipse size for the model. It the ellipse size is optimal, than the total number of errors is at a minimum, and all of the errors present are a result of model errors. Since only model errors are present, the number of type I and type II errors should be close to equal. Therefore, when the number of type I and type II errors are approximately equal, the ellipse size is near optimum and the total number of errors present is at a minimum for that model.

Examination of the footprint sets that resulted in errors hinted that a reduction in ellipse size of 15% would be a good starting point. The GAU model was reaccomplished

with ellipse dimensions based on 85% of the stick lengths. The results for each sortie are given in Appendix B. A summary of the results is provided in the table below.

Table 4-9. GAU Errors for Test Sorties / 85% Ellipse Size

	TYPE I	TYPE II
US-3RV	1	9
US-4RV	5	2

There was a small improvement in the overall model accuracy as the total number of errors went from nineteen to seventeen. The number of errors were divided fairly evenly between the US-3RV system and the US-4RV system, but there was a significant difference in the number of type I errors versus the number of type II. There were eleven type II errors compared to only six type I. This difference was especially significant for the US-3RV system, where nine of the ten errors were type II. This is an indication that the ellipse size may have been reduced too much. The model was run a third time with the footprint ellipse size set to 90% of the respective stick lengths. The specific results for each sortie are listed in Appendix B. The error breakdown was:

Table 4-10. GAU Errors for Test Sorties / 90% Ellipse Size

	TYPE I	TYPE II
US-3RV	3	4
US-4RV	6	2

Using the 90% ellipse size, there were a total of 15 errors out of the eighty test sorties, for an accuracy of 81.2%. The larger number of type I errors compared with the type II indicate that the optimum ellipse size must be based on between 90% and 85% of the stick lengths. It is not necessary to precisely fix the ellipse size to this particular data set, since the optimum ellipse dimensions may vary somewhat with different missile systems and different target arrays. The goal of this research is to find a value that will yield good results for all missile systems and target arrays. It is important to recall that the 81.2% accuracy achieved here was accomplished using borderline sorties that challenge the model. A total enumeration of all the possible DGZ combinations would include large numbers of easily classified sorties and the accuracy figure would be much higher.

Energy Space Transformation Model Testing

In order to have a valid comparison between the GA model and the EST model, the same eighty test sorties were used to test both models. The scaling factors, *a* and *b*, were set equal to the down and cross range stick lengths, respectively. Equations (3-7) and (3-8) were used to compute the down and cross range energy distance from each DGZ in a sortie to the focal point DGZ. The energy distance from each DGZ to the focal point DGZ was then found using the Pythagorean theorem. These energy distances were then summed to get the PBV fractional energy (PFE) for the sorties. If the PFE for a sortie was less than one, then the sortie was classified as feasible.

Optimal focal point. Changing the focal point DGZ for a sortie changes the value of the PFE for the sortie. When the EST model is applied in WAM, all DGZs in a sortie will be considered as potential focal points. A sortie is found to be feasible as long as there is at least one DGZ that can provide a focal point that yields a PFE less than one. If no such DGZs exist, then the sortie is classified infeasible. Therefore, it was necessary in the testing of this model to try each DGZ in a sortie as the missile focal point. The focal point that gives the lowest PFE is defined as the optimum focal point. The optimal focal point was always a DGZ that was centrally located with respect to the others. Focal points located on the fringes of the footprint generally yield higher energy totals since the sum of the distances to the other DGZs is greater. The energy data listed for the test sorties in this research is based on using the optimal focal point for each test sortie.

Preliminary results. The appropriate range-to-first-target, R, was used in the linear regression approximations for the stick lengths given in Table 4-4. The scaling factors, a and b, were then set equal to the resulting stick length values, and used in equations (3-7) and (3-8). (Note that the scaling factors a and b used in the EST model are calculated using the full stick length values, as opposed to the ellipse semi-major and semi-minor axes, p and q, used in the GA model, which are calculated using half of the stick length values). The results for the eighty test sorties are shown in Appendix C. The results are summarized in Table 4-11.

There were a total of thirteen errors for the eighty sorties, which is an accuracy of 83.7%. Listed in Appendix C along with the classification of each sortie by

Table 4-11. EST errors for Test Sorties

	TYPE I	TYPE II
US-3RV	4	2
US-4RV	1	6

the EST model is a column listing the PFE for each sortie. It is encouraging to note that there were many cases where the model not only classified the sortie correctly, but also matched the *PBV fuel remaining* value output by MPS to within a few percent. Sorties 4, 22, 38, 49, and 75, for example, all had PFE values from the EST model that were within 3 percentage points of the corresponding *%PBV fuel remaining* value from MPS. The PFE also is useful for determining the margin of error when sorties are misclassified. Several of the sorties that were misclassified missed by a very slim margin. MPS, for example, found sortie 2 to be infeasible. EST misclassified the sortie as feasible, but the PFE value of 0.998835 shows that the model came very close to correctly classifying the sortie. Sortie 19 provides another example. MPS found sortie 19 to be feasible, using 98% of the PBV fuel. Although the EST model misclassified the sortie as infeasible, it came close to the 98% figure by predicting it would take 100.5655% of the PBV energy to strike all of the DGZs. Sorties 24, 43, 65, 69, and 79 were also misclassified as infeasible, but they were all within 3 percentage points of the PBV energy.

Optimizing EST. Because the margin of error was so slim on several of the misclassified sorties, it was apparent that the total number of errors is very sensitive to the values chosen for *a* and *b*. Slight changes in either of these values may have a large

impact on the model results. To investigate this further, the spreadsheet used for the model was modified to output the total number of errors as the linear regression parameters in Table 4-4 were changed. The goal was to minimize the total number of errors produced by the model by changing the variables β_d and β_c, which are the y intercept parameters for the down range and cross range linear regression equations, respectively. It was decided to vary only the y intercept parameters and not the slope parameters in order to change the scaling factors uniformly throughout the spectrum of missile ranges. This minimization could not be accomplished using linear programming because the energy constraints are based on elliptical equations and are therefore nonlinear.

For this analysis the two missile systems were treated separately for two reasons. First, the error distribution produced by the first run indicates that the US-3RV system needs the scaling parameters to be decreased, while the US-4RV system needs them increased. (Interestingly, this is the opposite of what was encountered with the geometric approximation model.) And second, each system has its own distinct stick lengths and linear regression equations to approximate them.

By changing the values for β_d and β_c in very small increments, it was possible to observe the corresponding change in the values for the PFE for each sortie. If the DGZ locations for a sortie are held constant, then reducing the dimensions of the ellipse causes the PFE value to increase, while increasing the dimensions reduces the PFE value. The parameters were adjusted in such a way that the PFE values for misclassified sorties were shifted toward one. Consider for example sortie 2 of the US-3RV system. This sortie

66

would no longer be in error if the ellipse size were reduced slightly to increase the PFE value from 0.998835 to a value greater than one. But adjusting the regression parameters in such a fashion caused all of the PFE values for that missile system to increase. This inevitably caused some properly classified sorties to shift toward becoming misclassified. Sortie 38, for example, was properly classified as feasible with a PFE of 0.946663. As the ellipse dimensions were reduced to correct type I errors such as sortie 2, sortie 38, among others, shifted toward becoming a type II error. By carefully manipulating both the down and cross range parameters, sorties that were misclassified could be corrected while avoiding forcing other sorties to become errors. Using this technique, the combination of the parameters were adjusted until the least possible number of errors were present. The sortie results with the new values for β_d and β_c are given in Appendix C. There were a total of only eight errors for an accuracy of 90%. The resulting error distribution was:

Table 4-12. EST errors for Test Sorties, Optimized Ellipse Dimensions

	EST Errors	
	TYPE I	TYPE II
US-3RV	0	3
US-4RV	2	3

The parameters that produced the above results are:

Table 4-13. Optimal Regression Parameters for EST

y Intercept Parameter

	β_d	β_c
US-3RV	-795	160
US-4RV	-863	170

These parameters were then used to reconstruct the linear regression models for the down and cross range stick lengths to be used for calculating the scaling parameters for the EST model. The optimized equations are given in Table 4-14.

Table 4-14. Optimal Regression Equations for EST

	Down Range	Cross Range
US-3RV	$0.63R$-795	$0.063R$+160
US-4RV	$0.75R$-863	$0.081R$+170

A comparison of these regression lines with the actual stick length plots provides an indication of how accurate stick length is for determining the scaling parameters, a and b. The following plots show the down range and cross range stick length curves for each system, overlaid with the regression lines that provided the least number of EST errors.
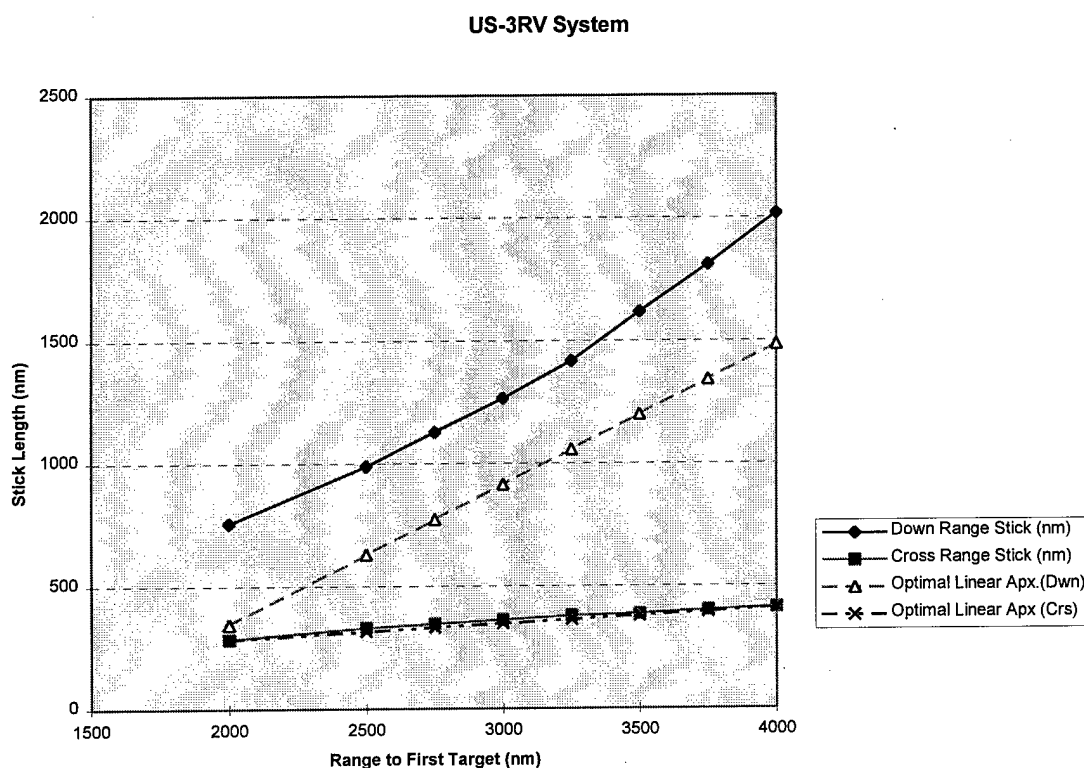
US-3RV System

Figure 4-8. Optimal Regression vs Stick Length, US-3RV
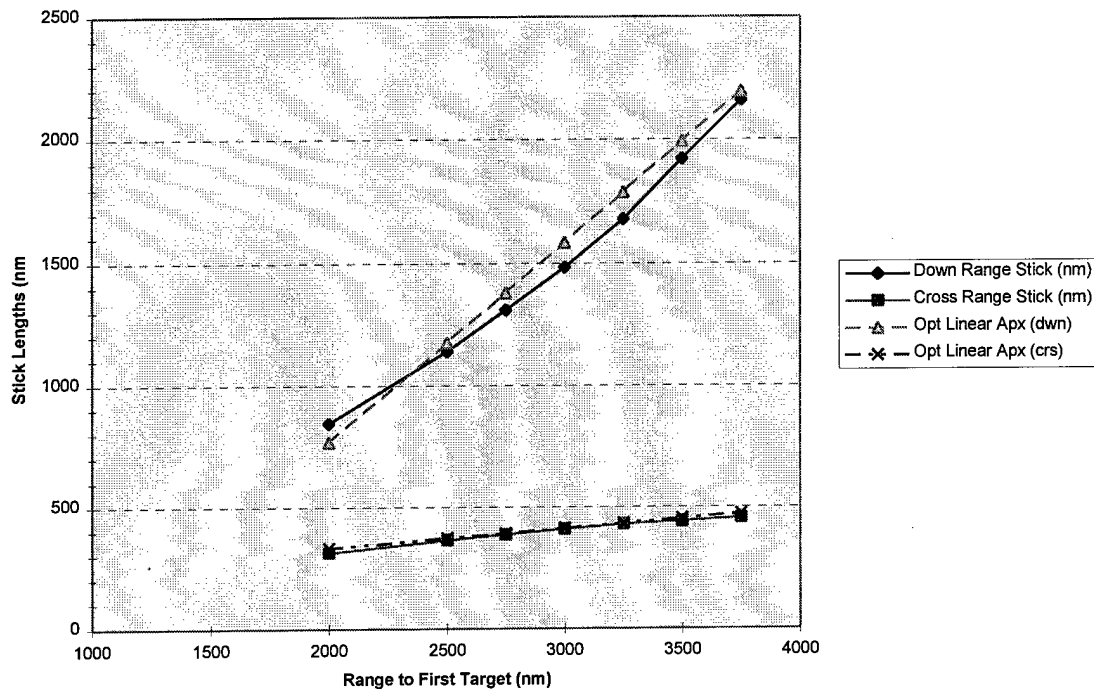
Figure 4-10. Optimal Regression vs Stick Length, US-4RV

For both missile systems, the cross range stick length was an extremely accurate

model for the optimum cross range scaling parameter. For the down range scaling

parameter, Figure 4-9 shows that the down range stick length was too large to give the

lowest possible number of errors for the US-3RV system. Reducing the a value below

that dictated by the down range stick length resulted in only three errors out of the forty

test sorties for the US-3RV system. However, using the original linear regression

equation for the down range stick length gave only five errors, and it was possible to

achieve four errors with only slight deviations from the original equation. Thus, although

the optimum model performance for this system came with a significant reduction in the

value of *a*, the original stick length linear regression equation provided good performance. For the US-4RV system, only slight changes from the original linear regression equations were needed to reduce the number of errors from seven to five. The line approximating the down range stick length had to be shifted down by 52 nm, while the line approximating the cross range stick length was shifted up 13 nm. This confirms the hypothesis that the number of errors produced is sensitive to small changes in the scaling parameters. However, the plot in Figure 4-10 shows that although slight changes in the scaling parameters effects the number of errors, the optimum scaling parameters are very close to those achieved by using a linear regression approximation of the stick lengths.

Launch Site Division

To this point, it has been assumed that a launch site is a single point from which the missile sorties originate. In actuality, a missile field is not a single point, but a series of many collocated missile silos. The dimensions of a typical missile field can exceed one hundred nautical miles in length or width. Therefore, to properly implement these models, it must be determined how large a launch site can be before a second launch site must be defined in order to maintain the accuracy of the models. If the launch site definition is too large, then errors are introduced since sortie launch azimuth and range data may be incorrect. If the launch site definition is too small, then the number of ellipses to be computed could be unnecessarily large.

Sorties 41 through 80 were used in conjunction with the energy space

transformation model to study this problem. First, all data for the sorties was held

constant while the launch azimuth was changed in one degree increments. This had the

effect of slowly moving the launch site laterally with respect to the target area. As the

launch site was moved, the effect on the number of errors produced by the model was

recorded. Figure 4-11 shows a plot of the launch azimuth vs the number of errors

produced by the model. This data was collected while using the optimum values for the

ellipse parameters.

US-4RV Errors vs Change in Launch Azimuth
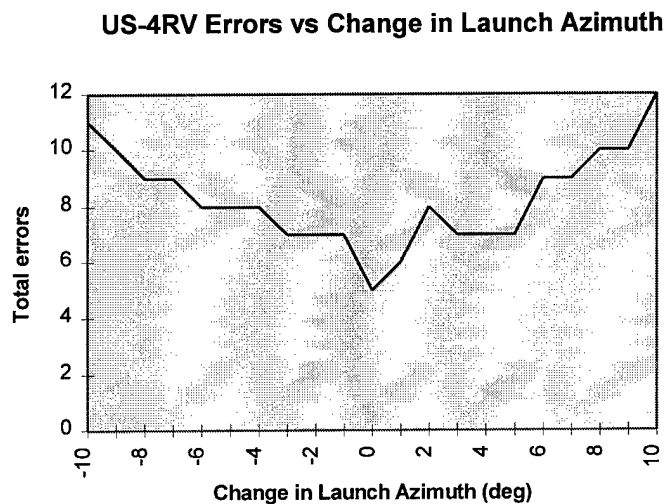
Figure 4-11.

The important aspect of the curve in Figure 4-11 is its slope, as this shows how

sensitive the model is to changes in launch azimuth. The steeper the slope, the greater the

change in the number of errors produced by the models per degree change in launch

azimuth. The steepest slope in the plot is two, which means in the worst case two errors

were induced per degree change in launch azimuth. Therefore the launch azimuth should

72

be able to change by a value of 0.5 degrees without affecting the model accuracy. The average range-to-first-target for these forty sorties was 3940 nm. At that range, 0.5 degrees of launch azimuth corresponds to 34.4 nm. Thus, the width of a launch site can extend 34.4 nm to either side of the center point without affecting the models. Here, the term "width" refers to the lateral dimension with respect to the general direction of the launch azimuth. The length of the launch site is not critical as the models are far less sensitive to slight changes in range. It should be pointed out that the 0.5 degree figure is primarily dependent on the DGZ density of the target area for the sorties at the launch site. A target area is said to have high DGZ density if there are a relatively large number of DGZs per unit area. If the target area is very dense, then it is likely that slight realignments of ellipses due to changes in azimuth would change the set of enclosed DGZs. In sparse target areas, it is less likely that the realignment of an ellipse would enclose new DGZs or exclude ones that were originally included. Thus, when this model is applied to real world data, variations in the DGZ density of the target area may affect the applicability of the 0.5 degree figure. But since the target area is not known in advance of running WAM, 34 nm, which corresponds roughly to the size of one US missile squadron, should be acceptable in most cases. This figure is also based on the average range-to-first-target for the missiles at a particular launch site. As a rule of thumb, if the expected average range-to-first-target is expected to change significantly from the 3490 nm used here, the total width of a launch site can be calculated by multiplying the expected average range-to-first-target for the launch site by $\pi/180$.

73

Submarine Patrol Areas

The footprinting problem for submarines provides a unique challenge because the exact launch site for a Submarine Launched Ballistic Missile (SLBM) cannot be pinpointed. Submarines are assigned large patrol areas, and are expected to be able to successfully complete all of their assigned sorties from any point within the patrol area. Thus, there are an infinite number of potential launch points within the patrol area. The patrol areas are far too large to be classified as one launch site, so a means of modeling all of the potential launch sites within the patrol area is needed. This can be accomplished by using the extreme points of the launch area. The extreme points of the patrol area can each be considered as a launch site for the missile sorties belonging to the respective submarine. As long as the patrol area is a convex area, then if a sortie is feasible from all of the extreme points, it is feasible from any point within the convex region. Therefore, SLBM sorties would be modeled more restrictivly, as they must be classified as feasible from several different launch points before the model can classify the sortie as feasible.

Summary

Initial testing of the geometric approximation model found that it was not flexible enough because of its requirement for the focal point DGZ to be the ellipse centroid DGZ. The unhinged version of the model does not fix the focal point DGZ at the centroid, but allows any DGZ in a sortie to be focal point. The flexibility of the unhinged geometric approximation model greatly improved its performance. From this point forward, when referring to the GA model, it is assumed to be the unhinged version.

Testing of the energy space transformation model showed that the model, when used with the stick length assumption, is sound. The results of the model using the optimized values of a and b show that EST can successfully model MIRV footprints. The specific values for the scaling parameters were tailored to this test data, and the optimal values may vary with respect to PBV stick lengths when applying this model to real world data. However, the stick lengths provided an excellent approximation in all test cases, and the results using stick lengths to set the scaling parameters were acceptable.

V. Verification

Introduction

In this chapter, the two footprinting models are verified by testing them with a missile system with different capabilities than those used to develop the models.

Model Verification

In order to verify the models that were developed in Chapter IV, a new missile system was assembled. Since WAM must deal with missile systems with various numbers of warheads, the verification should demonstrate how the footprinting models handle a system with a different number of MIRVs than those used to develop and test the models. Therefore, a third missile system was created with five MIRVs. The MIRVs were of the same specifications as those carried on previous systems. The added weight of the fifth MIRV reduces the maximum range of the system to a level where it could no longer reach the majority of the targets from either launch site; therefore a new booster was created. The new booster had specifications similar to the previous booster, except the second stage was given an increase in thrust of 44,000 pounds. The resulting system had a maximum booster range of 5299 nm. Launch site 2 was selected as the base for the US-5RV system in order to put the majority of the DGZs in the heart of the range envelope. In many cases, the test sorties were flown near the range limits of their respective systems. In case that had some effect on the results of the model testing, the

verification sorties were flown at booster ranges well below their maximum.

In order to provide the PBV with sufficient energy to disperse the five MIRVs enough to have a large number of DGZ targeting options, the following values were used to model the US-5RV PBV.

Table 5-1. US-5RV PBV Parameter Comparison.

Parameter	US-3RV	US-4RV	US-5RV
Usable Fuel Weight (lb)	1394	1800	2100
Axial Engine Thrust (lb)	165.6	200	350
Specific Impulse (sec)	306.6	320	380

The upgraded US-5RV PBV, along with the more powerful booster, gives the US-5RV system a greater MIRV dispersion capability than the previous two systems. The increased capability of this system provides not only a verification of the models, but also a test of how they can handle missile systems with larger footprints with respect to the target area. Figure 5-1 shows the stick length curves for the US-5RV system.

Stick Lengths for US-5RV System
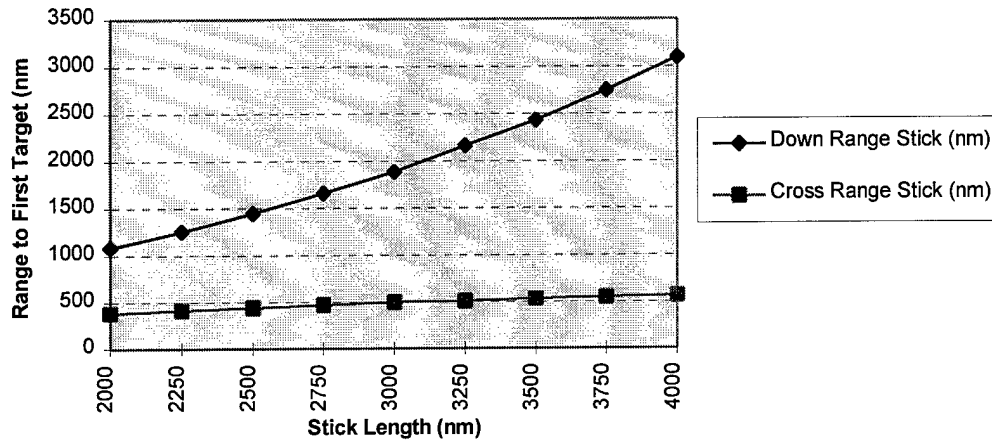
Figure 5-1. US-5RV Stick Length Curves.

Verification Sorties. Twenty-five five-DGZ sorties were built using the same procedures used to build the original eighty test sorties. These sorties were chosen to be close to the border between feasible and infeasible. Table 5-2 lists the DGZ combinations for the twenty-five verification sorties.

These twenty-five sorties were then tested for feasibility using MPS. For each sortie, every possible DGZ sequence was tried. If a sortie had any sequence that produced a feasible result, then that sortie was classified as feasible. The MPS results are given in Table 5-4, along with the % PBV fuel remaining.

Table 5-2. Verification Sorties

SORTIE #					
1	AL	L	AM	M	Q
2	AL	M	AC	L	AN
3	AL	L	AM	M	AC
4	BA	AE	J	F	BB
5	AD	AB	Z	K	AJ
6	BC	AR	B	BD	AS
7	T	V	U	O	P
8	X	V	Y	W	U
9	AE	BB	H	AU	Z
10	Z	AD	AJ	J	AU
11	AH	AG	AI	AS	AF
12	BD	B	C	AS	AR
13	B	D	AZ	AF	AQ
14	B	C	AW	AF	AQ
15	Q	M	N	R	S
16	BD	AG	AZ	AF	AS
17	AH	AG	AZ	AT	AQ
18	AU	AB	AD	AV	AX
19	M	Q	R	AL	AP
20	AE	AD	AA	F	E
21	AS	BC	BD	AQ	AT
22	AE	AD	AC	BA	F
23	AM	L	K	AO	AP
24	BB	AY	AX	F	H
25	M	AL	AM	AC	AA

GA model Verification. Using the methodology developed in Chapter III and refined in Chapter IV, the geometric approximation model was used to classify the verification sorties. First, the linear regression approximations for the stick lengths were used to get stick length values for each DGZ based on its range from the appropriate

79

launch site. These equations are given in Table 5-3. Next, ellipse semi-major and semi-minor axes were computed by dividing the respective stick length by two and

Table 5-3. Linear Regression Approximations for US-5RV Stick Lengths

	Down Range	Cross Range
US-5RV	R-1025	$0.091R$+217

multiplying by 0.9. The resulting values for p and q were then used in equation (3-1) to compare each DGZ with each ellipse. If a DGZ was included in an ellipse, then that DGZ was added to the footprint set for that ellipse. The complete list of footprint sets for the US-5RV system is included in Appendix D. The unhinged version of the model was used to build the footprint sets. Recall that when referring to the GA model it is assumed to be the unhinged version. GA had only one type II and two type I errors, for an overall accuracy of 88%.

EST Model Verification. The energy space transformation model was used to evaluate the verification sorties using the equations in Table 5-3 to compute the scaling factors, a and b, for each DGZ. These scaling factors were used in equations (3-6) and (3-7) to compute the PFE for each sortie. All five DGZs were tried as the focal point for

Table 5-4. Verification Sortie Results

Sortie #	MPS / %REM	GA / 0.9	EST	PFE
1	Y/13	Y	Y	0.89
2	Y/6	Y	Y	0.81
3	Y/11	Y	Y	0.872
4	Y/39	Y	Y	0.523
5	Y/26	Y	Y	0.996
6	Y/17	Y	*N*	1.068
7	Y/34	*N*	*N*	1.207
8	Y/7	Y	*N*	1.183
9	N	*Y*	N	1.171
10	N	N	N	1.375
11	N	*Y*	N	1.227
12	N	N	N	1.352
13	N	N	N	1.618
14	N	N	N	1.869
15	N	N	N	1.494
16	N	N	N	1.833
17	N	N	N	1.63
18	N	N	N	1.589
19	N	N	N	1.158
20	N	N	N	1.362
21	N	N	N	1.422
22	N	N	N	1.447
23	N	N	N	1.807
24	N	N	N	1.574
25	N	N	N	1.377

each sortie, and if any DGZ produced a PFE value of less than one, then that sortie was

classified feasible. The minimum PFE values obtained for each sortie are shown in Table

5-4. The EST model had an overall accuracy of 88% with only three type II errors.

Summary

A new missile system was used to verify the performance of both models using different missile data and a different number of MIRVs than those used for model development. Twenty-five five-DGZ sorties were chosen using the same technique used to choose the original test sorties. The model results were compared with MPS results for the same sorties. The comparison showed that both models were 88% effective in classifying the twenty-five verification sorties.

VI. Conclusions and Recommendations

Introduction

This chapter analyzes the results from the previous chapters. Three options for applying the models are presented. The strengths and weaknesses of each model are then reviewed. Based on the advantages and disadvantages of each model and the current force structure, a recommendation is given for the use of the models in WAM.

Options

The three best options available to incorporate the models presented in this research into WAM are:

1) Use the geometric approximation model exclusively. (From this point forward it is assumed that the geometric approximation model is the unhinged version). This would involve integrating the GA constraints given in Chapter III into the WAM formulation.

2) Use the energy space transformation model exclusively. This would involve integrating the EST constraints given in Chapter III into the WAM formulation.

3) Use the energy space transformation model within WAM as a part of the optimization process, but employ the geometric approximation model as a preprocessor. Using this technique, the GA model ellipses can be used prior to running WAM to eliminate a large number of decision variables. The remaining decision variables are

included in WAM and would be subject to the EST footprinting constraints that were presented in Chapter IV.

Preferred Error Types

As discussed in Chapter IV, there are two types of errors a model can produce; type I errors occur when the model gives a false feasible result, and type II errors occur when the model gives a false infeasible result. Which of the two types is produced more frequently by a model can be controlled by adjusting the model parameters. This is advantageous in the application of the models since one error type is preferred over the other depending on the circumstances. Which error type is preferred depends on how the models are integrated into WAM. If the model footprint constraints are to be integrated into WAM as a part of the optimization process, then type II errors are preferred to type I errors. This is because when the footprint constraint in WAM classifies a sortie as infeasible that in reality could have been completed by the PBV, the constraint is being more restrictive than the actual PBV footprint. This may cause WAM to make a weapon assignment that reduces the value of the objective function. A solution may be chosen that is slightly less than the optimal solution that could have been obtained within the limitations of the true footprinting capability of the PBVs. On the other hand, a type I error made by the WAM footprint constraints causes a weapon assignment to be made that is, in reality, infeasible. From a modeling standpoint, it is better to have a feasible solution with a Damage Expectancy (DE) slightly less than that which can actually be

achieved, than to have an infeasible solution with a higher DE than the missiles are capable of achieving.

Although type II errors are preferred during the optimization, type I errors are preferred during preprocessing. This is because when a model is being used as a preprocessor, its function is to pare down the number of decision variables in WAM by eliminating those that fail to constitute a feasible sortie. The remaining variables must then meet the footprint constraints during the WAM assignment process. When a type II error occurs during preprocessing, it rejects a feasible decision variable from the WAM formulation. This has the disadvantage of reducing the options available to WAM to achieve the best possible solution. However, in contrast to type I errors produced internal to WAM, type I errors produced during preprocessing are of little consequence as long as the decision variables are later subject to footprint constraints during the WAM assignment process. A type I error during preprocessing merely fails to screen an infeasible decision variable from being included in the WAM formulation.

Force Structure

The two models have different levels of performance depending on the number of reentry vehicles (RVs) carried by a missile system. Therefore, in order to make the best possible decision on how the models are to be incorporated into WAM, it is necessary to review the number of RVs carried by current weapon systems. Figure 6-1 shows the number of RVs carried by the missile systems in our current nuclear force structure (8). The most common number of RVs to be modeled is three. The section labeled "8 (4)"

refers to the Trident C-4 system, which currently carries eight RVs, but because of the

START II treaty, its RV carriage is expected to be reduced to four RVs (8:56).
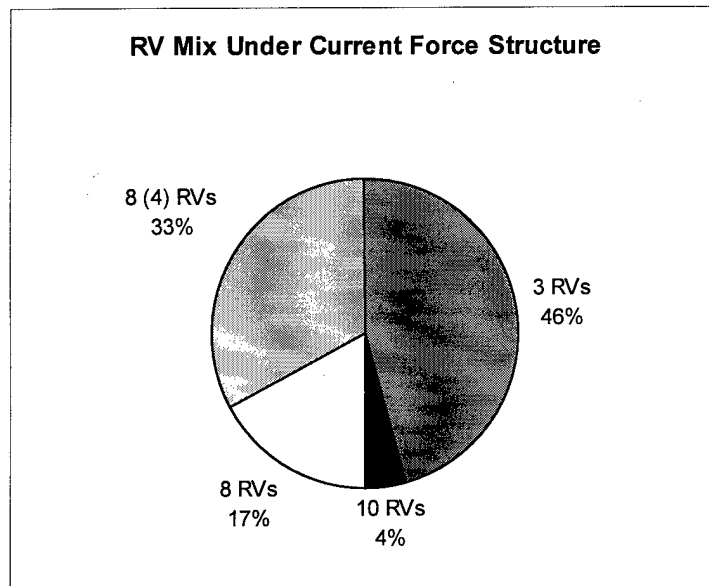
Figure 6-1. Number of RVs Carried per Booster

Strengths and Weaknesses

Now that the development, testing, and Verification of the models is complete,

several observations about the strengths and weaknesses of the models can be made.

Linear Arrangement of DGZs. Both GA and EST performed better on sorties

where the DGZ arrangement was more linear. The closer a sortie came to having the

DGZs in a straight line, whether in down range or cross range, the easier it was for the

models to correctly classify the sortie as feasible or infeasible. Conversely, both models

tended to struggle on sorties where the DGZs were arranged in a manner that approaches

a regular polygon. For example, both models failed to correctly classify Verification

sortie 7 as feasible. The relation between Verification sortie 7 and the missile flight path

is depicted in Figure 6-2 below. This is an example of a sortie where the DGZ pattern

forms close to a regular polygon.

Δ V

Δ U   Δ T

Missile
Flight Path   Δ O   Δ P
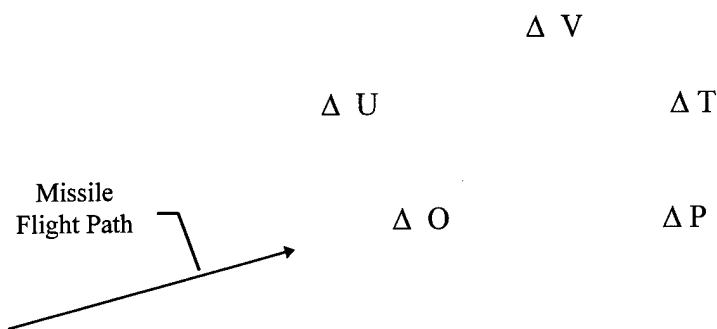
Figure 6-2. Verification Sortie 7

MPS found that the PBV could strike all five DGZs and still have 34% of its fuel

remaining. The GA model, however, could not find an ellipse that would enclose all five

DGZs. None of the five ellipses centered on the DGZs in this sortie could enclose both P

and U simultaneously. EST also misclassified the sortie. Since the DGZs are close to

being regularly spaced, each DGZ, when considered as the focal point, yields close to the

same PFE value for the sortie. If that value is well above one, there is no way for the

model to find a focal point DGZ that will yield a feasible sortie. DGZ T was found to be

the optimum focal point for Verification sortie 7, with a PFE of 1.2. (It was common for

the optimum focal point to be the DGZ farthest from the launch point, as this DGZ

requires the greatest time of flight, which gives the PBV the greatest MIRV dispersion

capability.)

DGZ density. The density of the DGZs in the target area has an effect on the accuracy of the GA model. Since this model relies on the placement of ellipses to enclose the DGZs of a feasible sortie, it is more likely that such an ellipse can be found if there are more ellipses present. Since each DGZ is the centroid of a footprint ellipse, there are more ellipses for the model to choose from in denser target areas. The accuracy of the EST model is unaffected by DGZ density.

Clusters of DGZs. When the DGZs in a sortie are distributed such that most are in a tightly packed cluster while one or two are widely scattered, the EST model is more accurate than the GA model. Because the EST model sums the energy distance from the focal point DGZ to all other DGZs, it is very accurate in cases where DGZs are tightly packed as long as the focal point DGZ is located in the cluster. Even if one distant DGZ is included in the sortie, the sum of the energy distance from each DGZ to the focal point is close to the energy distance from DGZ to DGZ in the actual sequence used by the PBV. The GA model, on the other hand, tends to produce type II errors for these sorties. This is because the ellipse dimensions are a function of the stick lengths, which are based on each MIRV receiving an equal amount of PBV energy. But MIRVs targeted into a tight cluster will use less than their share of PBV energy. This leaves the few remaining MIRVs with far more energy than their share, which gives them the potential to be displaced well outside the footprint ellipse.

Number of RVs. The EST model is less accurate for higher numbers of MIRVs because of the assumption that the total energy to complete a sortie can be approximated by summing the energy to displace each MIRV from the focal point DGZ. In actuality,

the energy used by the PBV is that required to maneuver from the focal point DGZ to the next DGZ in sequence, and from the next DGZ to the following DGZ in the sequence, and so forth until the sortie is complete. For the three RV case, the EST model is very accurate because the sum of the energy distances from the central DGZ to the other two DGZs is equal to the sum of the energy distances from DGZ 1 to DGZ 2 to DGZ 3. But this is only true in the three RV case. After that, each time a DGZ is added to the sortie, the difference between the PFE value produced by the model and the actual PBV energy used increases. Therefore, each additional RV adds more error to the model.

The RV mix given in Figure 6-1 for the current force structure shows that 47% of the sorties to be modeled carry three RVs, and within the next few years, up to 79% of the sorties may carry less than five RVs. This force structure does not warrant the rejection of the EST model.

The GA model, on the other hand, models MIRV footprints in a more general sense. Thus, the GA model should not suffer a decrease in accuracy as the number of MIRVs in a sortie increases. The results from the testing summarized in Table 6-1 below show that the GA model maintained consistent accuracy as the number of MIRVs were increased. So there is a tradeoff between the accuracy of the two models depending on the number of MIRVs being modeled.

Table 6-1. GA Model Accuracy versus Number of MIRVs

Number of MIRVs per Sortie	GA Model Accuracy (90% Ellipse Size)
3	85%
4	82.5%
5	88%

Recommendations

Based on the results of this research and the characteristics of the footprinting models presented, it is recommended that option c above be implemented. The energy space transformation model was more accurate for the sorties with three and four RVs, which will comprise at least 47% and possibly as much as 79% of the sorties WAM will assign over the next several years. Although the geometric approximation model performed well on the five RV Verification sorties, the requirement to include the integer variable, λ_{ij}, will make WAM more cumbersome to run than it would be with the EST constraints. However, WAM can be streamlined by using the GA model as a preprocessor to reduce the number of decision variables to be included in the formulation.

Recall that the WAM formulation using the EST model uses the decision variable y_{lij}, where y_{lij} is a binary variable indicating whether or not the jth DGZ is targeted by the lth booster with the ith DGZ as the missile focal point. Prior to running WAM, GA can be used to generate footprint sets. Since a footprint set is generated for each ellipse, and an ellipse is defined for each booster/DGZ combination, there will be a footprint set for all

combinations of l and i. Recall that boosters sharing the same launch site can use the same ellipses to reduce the required number of calculations. If the jth DGZ is not included in the li^{th} footprint set, than the variable y_{lij} is excluded from the WAM formulation.

This method of applying the two models has three major advantages. First, it requires a sortie to be classified as feasible by both GA and EST before that sortie can be assigned by WAM. This minimizes the number of type I errors that WAM will produce, since both models must generate a type I error for the same sortie in order for WAM to generate a type I error. This reduces the likelihood of infeasible sorties being assigned in the optimal solution. Second, the GA model has an influence on the footprint constraints without requiring the inclusion of additional integer variables. This makes it quicker and easier to reach an optimal solution. And third, preprocessing with the GA model significantly reduces the size of the WAM linear program, since many decision variables are not included that otherwise would have been if EST were used exclusively in the model.

Areas for Further Research

Sequencing. Most of the error in the energy space transformation model comes from summing the total energy distance from the focal point DGZ to all the other DGZs in a sortie. In reality, the PBV uses its energy to maneuver from DGZ to DGZ in sequence (see Figure 3-3). In order to use footprint constraints that account for the actual sequence in a sortie, two subscripts would have to be added to the decision variables.

The first subscript would designate the previous DGZ struck by the PBV, and the second would designate the subsequent DGZ to be struck by the PBV. Although this would make the EST model far more accurate, it would result in more decision variables than can be realistically dealt with. If it were possible to find a way to reduce the number of decision variables, yet account for the true sequencing of the PBV, then the EST model would be greatly improved.

Minimum time of flight. This research was done under the assumption that the missiles are fired on a maximum time of flight trajectory. Although this is valid most of the time, there are some missiles designated against time sensitive DGZs. Further research can be done to study the effect on the models of using the depressed minimum time of flight trajectory.

Summary

Based on the results of this research, MIRV footprints can be successfully modeled in WAM. By using a combination of the geometric approximation model as a preprocessor with the energy space transformation model integrated into the WAM formulation, an optimum weapons assignment can be realized that includes MIRV footprint constraints. The combination of the two models both reduces the size of the WAM formulation and number of infeasible sorties WAM will produce without causing a undue decrease in the DE due to rejecting a large number of feasible sorties. The integration of these models into WAM will provide a usable weapons assignment model that will improve USSTRATCOM's ability to target our strategic forces in an optimal manner.

Appendix A.

Appendix A contains the footprint sets for each run of the geometric approximation model. A footprint set is the set of all DGZs contained within a footprint ellipse generated by the GA model. All data presented in Appendix A was achieved using the unhinged version of the model. Each table is labeled with the missile system and the ellipse size used to construct the footprint sets. The ellipse size is given as a percentage of the linear approximation of the stick length that was used to calculate the ellipse parameters.

Table A-1.

US-3RV Missile System Footprint Set, 100% Ellipse Size. (Centroid DGZ is in Bold)

A	BC	AR	AQ	AS					
B	BB								
C	J								
D	AY	AX	AV	AU	AG	AH			
E	BD	AS	AF	H	G	BC			
F	BD	BA	AK	AJ	BB	AE			
G	E	A	L	I	H	BC			
H	G	E	L	I					
I	H	G	L	E	A	AM			
J	C	AB	AA	Z	AD				
K	F	BB	BA	Q	AE	AK	M		
L	I	H	G	P	T	E			
M	K	F	BA	S	AL	AK	AJ		
N	AP	AO	O	AN	AM	X	W	V	U
O	N	AM	V	X	K	U	L	I	
P	L	T	I						
Q	K	R	AD	AC					
R	Q	AD	AC						
S	M	AL	AK	AJ					
T	P	L	O						
U	O	N	Y	X	W	V	AN	AM	AO
V	U	O	N	X	AM				
W	U	N	Y	X					
X	W	V	U	O	N	Y	AM		
Y	X	W	U	N					

Z	J	AB	AA	AY	AV	AU
AA	Z	J	AB			
AB	AA	Z	J	C	AU	AV
AC	AB	R	Q	K	AD	
AD	AC	J	BB	AE		
AE	K	F	B	BB	BA	
AF	BD	AT	AS			
AG	AH	AZ	D			
AH	AG					
AI	AZ					
AJ	M	AL	AK	F	BA	
AK	AJ	M	AL	F	BA	
AL	AK	AJ	M	F		
AM	AL	O	N	AP	AN	I
AN	AM	N	AP	AO		
AO	AN	AP	N			
AP	AO	AN				
AQ	AR	BC	A			
AR	AQ	A				
AS	AF	BC	BD	AQ		
AT	AF					
AU	Z	AY	AX	AV	D	AB
AV	AU	Z	AY	AX	D	
AW	AZ	AX				
AX	AW	AV	AU	AG	AZ	AY	D	AH
AY	AX	AV	AU	D		
AZ	AW	AI	AH	AG	AX	
BA	AK	AJ	AE	BB	K	F
BB	BA	AE	B	K	F	
BC	AS	AQ	A	E		
BD	AT	AS	AF			

Table A-2.

US-4RV Missile System Footprint Set, 100% Ellipse Size. (Centroid DGZ is in Bold)

A	BD	B	BC	AF								
B	A	BD	AF	D	C	AY	AZ	BC				
C	B	BD	AY	AX	AW	D	A	AV				
D	C	B	BD	AZ	AY	AF	A	AX				
E	BB	BA	AE	H	F							
F	E	BB	BA	J	H	G	AE	AU				
G	BA	I	H	AE	G							
H	G	F	E	BA	AE	BB						
I	G	AP	AK	AJ	K							
J	H	F	E	BB	BA	AU	AE	AD	Z	G	AV	AB
K	I	AK	AJ	AD	AC	AA	AP					
L	AO	AN	AM	AL	M	AK	AP					
M	L	AN	AM	Q	AL	AK	AJ	AC				
N	T	P	O									
O	N	T	P									
P	O	N	T	S								
Q	M	L	R	AL	AM	AC						
R	Q	M	S	AL	AM	L						
S	P	N	O	R	T							
T	P	O	N									
U	V											
V	U	O										
W	Y	X										
X	W	Y	U									
Y	X	W										
Z	J	BA	AE	AD	AB	AA	K	F	G	H		
AA	Z	K	AD	AC	AB	AJ	I	AK				
AB	AA	Z	J	H	F	AE	AD	BA	G	K		
AC	AA	M	K	AL	AK	AJ	I	L				
AD	AB	AA	Z	K	J	H	AE	BA	AJ	F	I	G
AE	AD	AB	J	H	G	F	BB	BA	Z	AU		E
AF	A	BD	BC	AS	AR	B						
AG	AI	AH	AS	AF	BC							
AH	AG	AI	AT	AS								
AI	AH	AG										
AJ	AC	K	I	AP	AL	AK	AA	M	L			
AK	AL	AC	M	L	K	I	AP	AJ	AL			
AL	AK	AJ	AC	Q	M	L	AN	AM	AP			
AM	L	AO	AN									
AN	AM	L	AP	AO	AL							
AO	AN	AM	L									
AP	AK	I	AN									

AQ	AT	AS	AR						
AR	AF	AS	BC	AQ					
AS	AR	AQ	AF	BC					
AT	AQ								
AU	AE	BA	AW	AV	J	F	BB	E	AY
AV	AU	BB	AY	AX	AW	J	C	BA	F	E
AW	AV	AU	AY	AX	C	BB			
AX	AW	AV	AY	D	C	B	AU		
AY	AX	AW	AV	D	C	B	BD		
AZ	B	D	C	BD	AF	AG			
BA	AE	BB	J	H	G	F	E	AB	AD
BB	AE	AU	AV	BA	J	H	E	F	
BC	AF	AR	AS	A	BD				
BD	D	AF	AR	AS	BC	B	A		

Table A-3.

US-3RV Missile System Footprint Set, 90% Ellipse Size. (Centroid DGZ is in Bold)

A	BC	AR	AQ						
B	BB								
C	J								
D	AY	AX	AV	AU	AG				
E	BD	AS	AF	H	G				
F	BD	BA	AK	AJ		AE			
G	E	A	L	I	H	BC			
H	G	E	L	I					
I	H	G	L						
J	C	AB	AA	Z					
K	F	BB	BA	Q	AE	AC			
L	I	H	G	P	T				
M	K	F	BA	S	AL	AK	AJ		
N	AP	AO	O	AN	AM	X	W	V	U
O	N	AM	V						
P	L	T							
Q	K	R	AD	AC					
R	Q	AD	AC						
S	M	AL	AK	AJ					
T	P	L							
U	O	N	Y	X	W	V	AN	AM	
V	U	O	N	X	AM				
W	U	N	Y	X					
X	W	V	U	O	N	Y			
Y	X	W	U						
Z	J	AB	AA	AY	AV	AU			
AA	Z	J	AB						
AB	AA	Z	J	C	AU				
AC	AB	R	Q	K	AD	AA			
AD	AC	J	BB						
AE	K	F	B	BB	BA				
AF	BD	AT	AS						
AG	AH	AZ							
AH	AG								
AI	AZ								
AJ	M	AL	AK	F	BA				
AK	AJ	M	AL	F	BA				
AL	AK	AJ	M						
AM	AL	O	N	AP	AN	I			
AN	AM	N	AP	AO					
AO	AN	AP							
AP	AO	AN							
AQ	AR	BC							

AR	AQ	A					
AS	AF	BC					
AT	AF						
AU	Z	AY	AX	AV	D		
AV	AU	Z	AY	AX	D		
AW	AZ	AX					
AX	AW	AV	AU	AG	AZ	AY	D
AY	AX	AV	AU	D			
AZ	AW	AI	AH	AG			
BA	AK	AJ	AE	BB	K	F	
BB	BA	AE	B	K			
BC	AS	AQ	A				
BD	AT	AS	AF				

Table A-4.

US-4RV Missile System Footprint Sets, 90% Ellipse Size (Centroid DGZ is in Bold)

A	BD								
B	A	BD	AF	D	C				
C	B	BD	AY	AX	AW	D			
D	C	B	BD	AZ	AY	AF			
E	BB	BA	AE	H	F				
F	E	BB	BA	J	H	G	AE		
G	BA	I	H						
H	G	F	E	BA	AE				
I	G	AP	AK	AJ					
J	H	F	E	BB	BA	AU	AE	AD	Z	AB
K	I	AK	AJ	AD	AC	AA			
L	AO	AN	AM	AL	M	AK			
M	L	AN	AM	Q	AL	AK	AJ	AC	
N	T	P	O						
O	N	T	P						
P	O	N	T	S					
Q	M	L	R	AL					
R	Q	M	S						
S	P	N							
T	P	O	N						
U	V								
V	U								
W	Y	X							
X	W	Y							
Y	X	W							
Z	J	BA	AE	AD	AB	AA			
AA	Z	K	AD	AC	AB	AJ			
AB	AA	Z	J	H	F	AE	AD	BA	
AC	AA	M	K	AL	AK	AJ			
AD	AB	AA	Z	K	J	H	AE	BA	G
AE	AD	AB	J	H	G	F	BB	BA	E
AF	A	BD	BC	AS	AR				
AG	AI	AH	AS						
AH	AG	AI							
AI	AH	AG							
AJ	AC	K	I	AP	AL	AK			
AK	AJ	AC	M	L	K	I	AP	AN	AL
AL	AK	AJ	AC	Q	M	L	AN	AM	
AM	L	AO	AN						
AN	AM	L	AP	AO					
AO	AN	AM							
AP	AK	I							
AQ	AT	AS							
AR	AF	AS	BC						

AS	AR	AQ	AF	BC			
AT	AQ						
AU	AE	BA	AW	AV	J	F	BB
AV	AU	BB	AY	AX	AW	J	C
AW	AV	AU	AY	AX	C		
AX	AW	AV	AY	D	C	B	
AY	AX	AW	AV	D	C	B	
AZ	B	D					
BA	AE	BB	J	H	G	F	E
BB	BA	AV	AU	AE	J	H	F	E
BC	AS	AR	AF	BD			
BD	BC	AR	AF	B	A		

Table A-5.

US-3RV Missile System Footprint Set, 85% Ellipse Size. (Centroid DGZ is in Bold)

A	BC	AR	AQ			
B	BB					
C	J					
D	AY	AV	AU	AG		
E	AF	H				
F	BA	AK	AJ	AE		
G	E	A	L	I	H	
H	G	E	I			
I	H	G	L			
J	C	AB	AA			
K	BB	BA	AE			
L	I	H	G	P	T	
M	F	BA	S	AL	AK	AJ
N	AP	AO	O	AN	AM	W	U
O	N	AM	V			
P	L	T				
Q	K	R	AD	AC		
R	Q	AD	AC			
S	M	AL	AK	AJ		
T	P	L				
U	N	Y	X	W	V	AN	AM
V	U	O	N	AM		
W	U	N	Y	X		
X	W	V	U	O	N	Y
Y	X	W	U			
Z	J	AB	AA	AV	AU	
AA	Z	J	AB			
AB	AA	Z	J	C		
AC	R	Q	AD			
AD	AC	BB				
AE	K	F	BB	BA		
AF	BD	AT	AS			
AG	AH					
AH	AG					
AI	AZ					
AJ	M	AL	AK	F	BA	
AK	AJ	M	AL	F	BA	
AL	AK	AJ	M			
AM	O	N	AP	AN		
AN	AM	N	AP	AO		
AO	AN	AP				
AP	AO	AN				
AQ	AR	BC				

AR	AQ	A			
AS	AF	BC			
AT					
AU	Z	AY	AX	AV	D
AV	AU	Z	AY	AX	D
AW	AZ	AX			
AX	AW	AV	AG	AZ	AY	D
AY	AX	AV	AU	D	
AZ	AW	AI	AH	AG	
BA	AK	AJ	AE	BB	K	F
BB	BA	AE	B	K	
BC	AS	AQ	A		
BD	AS	AF			

Table A-6.

US-4RV Missile System Footprint Set, 85% Ellipse Size. (Centroid DGZ is in Bold)

A	BD								
B	A	BD	AF	D	C				
C	B	BD	AY	AX	AW	D			
D	C	B	BD	AZ					
E	BB	BA		H	F				
F	E	BB	BA	J	H	G	AE		
G	BA	I	H						
H	G	F	E	BA	AE				
I	G	AP	AK	AJ					
J	AU	BA	BB	Z	AB	H	F	AE	AD
K	I	AK	AJ	AD	AC	AA			
L	AO	AN	AM	AL	M	AK			
M	AL	AC	L	AN	Q	AK			
N	T	P	O						
O	N	T	P						
P	O	N	T	S					
Q	M	L	R	AL					
R	Q	M							
S	P								
T	P	O	N						
U	V								
V	U								
W	Y	X							
X	W	Y							
Y	X	W							
Z	J	BA	AE	AD	AB	AA			
AA	Z	K	AD	AC	AB	AJ			
AB	AA	Z	J		AE	AD	BA		
AC	AA	M	K	AL	AK	AJ			
AD	AB	AA	Z	K	J	H	AE	BA	G
AE	AD	AB	J	H	G	F	BB	BA	E
AF	A	BD	BC	AS	AR				
AG	AI	AH							
AH	AG	AI							
AI	AH	AG							
AJ	AC	K	I	AP	AL	AK			
AK	AJ		M	L	K	I	AP		AL
AL	AK	AJ	AC		M	L	AN	AM	
AM	L	AO	AN						
AN	AM	L		AO					
AO	AN	AM							
AP	AK	I							

AQ	AT							
AR	AF	AS	BC					
AS	AR	AQ	AF	BC				
AT	AQ							
AU	AE	BA	AW	AV	J	F	BB	
AV	AU	BB	AY	AX	AW		C	
AW	AV	AU	AY	AX	C			
AX	AW	AV	AY		C	B		
AY	AX	AW	AV	D	C	B		
AZ	B	D						
BA	AE	BB	J	H	G	F	E	
BB	BA	AV	AU	AE	J	H	F	E
BC	AS	AR	AF	BD				
BD	BC		AF	B	A			

Appendix B.

Appendix B contains the results of the geometric approximation (unhinged) model for the eighty test sorties.

Table B-1. GA Results (Errors are in Bold. 85% and 90% Refer to Ellipse Size)

Sortie #	Geo Apx Unhinged 85%	Geo Apx Unhinged 90%	MPS/ %REM	Sortie #	Geo Apx Unhinged 85%	Geo Apx Unhinged 90%	MPS/ %REM
1	Y	Y	Y/22	41	*Y*	*Y*	N
2	N	N	N	42	Y	Y	Y/11
3	Y	Y	Y/23	43	Y	Y	Y/10
4	Y	Y	Y/47	44	N	N	N
5	Y	Y	Y/18	45	Y	Y	Y/18
6	*Y*	*Y*	N	46	Y	Y	Y/29
7	N	N	N	47	Y	Y	Y/15
8	Y	Y	Y/37	48	Y	Y	Y/10
9	Y	Y	Y/.09	49	Y	Y	Y/32
10	Y	Y	Y/10	50	Y	Y	Y/2
11	Y	Y	Y/43	51	Y	Y	Y/28
12	Y	Y	Y/48	52	Y	Y	Y/1
13	Y	Y	Y/24	53	Y	Y	Y/30
14	*N*	Y	Y/21	54	Y	Y	Y/2
15	Y	Y	Y/26	55	Y	Y	Y/23
16	N	*Y*	N	56	N	N	N
17	*N*	*N*	Y/12	57	N	*Y*	N
18	N	N	N	58	Y	Y	Y/2
19	*N*	*N*	Y/2	59	Y	Y	Y/21
20	N	*Y*	N	60	Y	Y	Y/37
21	*N*	Y	Y/20	61	N	N	N
22	Y	Y	Y/27	62	Y	Y	Y/5
23	N	N	N	63	*Y*	*Y*	N
24	N	N	N	64	*Y*	*Y*	N
25	N	N	N	65	N	N	N
26	N	N	N	66	Y	Y	Y/9
27	N	N	N	67	Y	Y	Y/18
28	*N*	Y	Y/12	68	Y	Y	Y/9
29	*N*	Y	Y/19	69	*Y*	*Y*	N
30	*N*	*N*	Y/23	70	N	N	N
31	Y	Y	Y/26	71	Y	Y	Y/23
32	N	N	N	72	*N*	*N*	Y/3
33	Y	Y	Y/24	73	N	N	N

34	Y	Y	Y/8	74	*Y*	*Y*	N
35	N	N	N	75	Y	Y	Y/28
36	Y	Y	Y/20	76	Y	Y	Y/24
37	Y	Y	Y/43	77	Y	Y	Y/20
38	*N*	*N*	Y/6	78	Y	Y	Y/12
39	Y	Y	Y/5	79	*N*	*N*	Y/3
40	*N*	*N*	Y/2	80	Y	Y	Y/21

Appendix C.

Appendix C contains the results of the energy space transformation model testing for the eighty test sorties.

Table C-1. EST and Optimized EST Results. (Errors are in Bold)

Sortie	Energy Space Transformation	PFE	Optimized EST	PFE	MPS/ %REM
1	Y	0.5433	Y	0.7001	Y/22
2	Y	0.9988	N	1.1089	N
3	Y	0.7331	Y	0.7446	Y/23
4	Y	0.4374	Y	0.5281	Y/47
5	Y	0.806	Y	0.9999	Y/18
6	N	1.0663	N	1.2389	N
7	N	1.2776	N	1.3647	N
8	Y	0.4411	Y	0.5192	Y/37
9	*N*	1.2538	*N*	1.2829	Y/0.09
10	Y	0.8274	Y	0.8325	Y/10
11	Y	0.519	Y	0.5262	Y/43
12	Y	0.4045	Y	0.4294	Y/48
13	Y	0.5738	Y	0.6351	Y/24
14	Y	0.6851	Y	0.814	Y/21
15	Y	0.5634	Y	0.7462	Y/26
16	N	1.3201	N	1.5148	N
17	Y	0.9155	Y	0.9943	Y/12
18	*Y*	0.8413	N	1.0004	N
19	*N*	1.0057	*N*	1.2258	Y/2
20	*Y*	0.8321	N	1.0291	N
21	Y	0.5816	Y	0.6967	Y/20
22	Y	0.7233	Y	0.8442	Y/27
23	N	1.5754	N	1.7322	N
24	*Y*	0.9661	N	1.0483	N
25	N	1.5778	N	1.5985	N
26	N	1.979	N	1.9907	N
27	N	1.0323	N	1.0624	N
28	Y	0.8383	Y	0.8804	Y/12
29	Y	0.7597	Y	0.8373	Y/19
30	Y	0.7399	Y	0.9778	Y/23
31	Y	0.611	Y	0.7041	Y/26
32	N	1.6274	N	1.6314	N
33	Y	0.6386	Y	0.7107	Y/24
34	Y	0.6737	Y	0.7699	Y/8
35	N	1.0813	N	1.3212	N

36	Y	0.7198	Y	0.7858	Y/20
37	Y	0.5396	Y	0.5976	Y/43
38	Y	0.9467	*N*	1.3124	Y/6
39	Y	0.8845	Y	0.9782	Y/5
40	Y	0.6614	Y	0.8563	Y/2
41	N	1.0034	*Y*	0.9762	N
42	Y	0.822	Y	0.8026	Y/11
43	Y	0.7296	Y	0.7092	Y/10
44	N	1.0199	N	1.0001	N
45	Y	0.9901	Y	0.9578	Y/18
46	Y	0.6406	Y	0.6164	Y/29
47	Y	0.6731	Y	0.6572	Y/15
48	Y	0.7141	Y	0.6993	Y/10
49	Y	0.653	Y	0.633	Y/32
50	*N*	1.0108	Y	0.9866	Y/2
51	Y	0.5401	Y	0.5225	Y/28
52	Y	0.8918	Y	0.871	Y/1
53	Y	0.7892	Y	0.7708	Y/30
54	Y	0.8436	Y	0.8112	Y/2
55	Y	0.675	Y	0.658	Y/23
56	N	1.3787	N	1.3328	N
57	N	1.0449	N	1.0175	N
58	Y	0.8783	Y	0.8508	Y/2
59	Y	0.7039	Y	0.6771	Y/21
60	Y	0.6992	Y	0.6831	Y/37
61	N	1.1837	N	1.1522	N
62	*N*	1.0898	*N*	1.0433	Y/5
63	N	1.1167	N	1.0847	N
64	*Y*	0.9928	*Y*	0.9693	N
65	N	1.0445	N	1.0162	N
66	*N*	1.0717	*N*	1.037	Y/9
67	Y	0.7963	Y	0.7706	Y/18
68	*N*	1.03	Y	0.9989	Y/9
69	N	1.1796	N	1.1428	N
70	N	1.6465	N	1.5915	N
71	Y	0.8735	Y	0.8509	Y/23
72	*N*	1.1849	*N*	1.1515	Y/3
73	N	1.0649	N	1.035	N
74	N	1.5325	N	1.4801	N
75	Y	0.7082	Y	0.6913	Y/28
76	Y	0.8194	Y	0.7945	Y/24
77	Y	0.9865	Y	0.9576	Y/20
78	Y	0.8669	Y	0.8395	Y/12
79	*N*	1.0278	Y	0.9983	Y/3
80	Y	0.7241	Y	0.7071	Y/21

108

Appendix D.

Appendix D contains the footprint sets for the US-5RV missile system used for verification.

Table A-9.

US-5RV Missile System Footprint Set, 90% Ellipse Size (Centroid DGZ is in Bold)

A	BD	BC	AR	AF	B							
B	A	BD	BC	AZ	AY	AX	AR	AF	D	C		
C	B	A	BD	AZ	AY	AX	AW	AV	D			
D	C	B	A	BD	BC	AZ	AY	AX	AF			
E	BB	BA	AE	H	G	F						
F	E	BB	BA	AU	J	H	G	AE				
G	F	E	BA	I	H	AE						
H	G	F	E	BB	BA	I	AE	AD				
I	H	G	AK	AJ	K							
J	H	G	F	E	BB	BA	AV	AU	AE	AD	AB	Z
K	I	G	AP	AL	AK	AJ	AD	AC	AA			
L	AP	AO	AN	AM	AL	Q	M	AK	AJ			
M	L	AP	AO	AN	AM	R	Q	AL	AK	AJ	AC	
N	T	P	O									
O	N	T	P	V								
P	O	N	T	S	AO	AM						
Q	M	L	R	AN	AM	AL	AK	AC				
R	Q	M	L	S	AM	AL						
S	R	P	O	N	T	AO	AM					
T	S	P	O	N	V							
U	X	V										
V	U	T	O	X								
W	U	Y	X									
X	W	V	U	Y								
Y	X	W										
Z	K	J	H	G	F	BB	BA	AE	AD	AB	AA	
AA	Z	K	I	G	AD	AC	AB	AK	AJ			
AB	AA	Z	K	J	H	G	F	BB	AE	AD	BA	
AC	AA	Q	M	L	K	I	AP	AL	AK	AJ		
AD	AB	AA	Z	K	J	I	H	G	F	AJ	AE	BA
AE	AD	AB	Z	J	H	G	F	E	BB	BA	AU	
AF	B	A	BD	BC	AS	AR						
AG	AF	AI	AH	BC	AZ	AS	AR					
AH	AG	AI	AT	AS	AQ							
AI	AH	AG	AF	AS								
AJ	AD	AC	AA	M	L	K	I	G	AP	AL	AK	
AK	AJ	AC	M	L	K	I	AP	AN	AL			
AL	AK	AJ	AC	Q	M	L	K	I	AP	AO	AN	AM
AM	AL	L	AO	AN								

AQ	AT	AS	AR								
AR	AQ	AF	AS	BD	BC						
AS	AR	AQ	AF	BD	BC						
AT	AQ										
AU	AE	BA	AY	AX	AW	AV	J	F	E	C	BB
AV	AU	AE	BB	BA	AY	AX	AW	J	F	E	C
AW	AV	AU	BB	AY	AX	D	C	B			
AX	AW	AV	AU	BD	BB	AY	D	C	B		
AY	AX	AW	AV	AU	A	BD	D	C	B		
AZ	AY	AG	AF	B	BD	BC	D	C			
BA	AU	AE	AD	AB	Z	BB	J	H	G	F	E
BB	BA	AV	AU	AE	J	H	G	F	E		
BC	AS	AR	AQ	AF	A	BD					
BD	BC	AS	AR	AF	D	C	B	A			

110

Bibliography

1. Department of the Air Force, *Air Navigation,* AFM 51-40, (C2), Washington: HQ USAF, 2 January, 1989.

2. Ayres, Frank Jr., and Elliott Mendelson, *Differential and Integral Calculus*, McGraw-Hill, 1976.

3. Bate, Roger R., Donald D. Mueller, and Jerry E. White, *Fundamentals of Astrodynamics*, Dover, New York, 1984.

4. Gallagher, Mark A., and Jeffrey D. Weir, *An Alternative Weapons Allocation Methodology*, Presentation for the Military Operations Research Symposium, 19 June, 1996.

5. Gallagher, Mark A., *Weapons Allocation Model (WAM),* WAM overview used at the 64th MORS Symposium, 19 June, 1996.

6. Gallagher, Mark A., USSTRATCOM J5 Analyst, Personal Interview, 7 August, 1996.

7. Gallagher, Mark A., USSTRATCOM J5 Analyst, Telephone Interview, 22 October, 1996.

8. Lennox, Duncan, ed., *Jane's Strategic Weapons Systems*, Jane's Information Group, Alexandria VA, 1996.

9. Langley, R. Warren, and Dana Billings, *Multiple Independently Targeted Reentry Vehicle (MIRV) Targeting Models*, Frank J. Seiler Research Laboratory Project 2304, Final Report, August 1980, DTIC AD-AO90 151.

10. *MIRV Footprint Theory Study*, Volume I, Office of the Chief of Naval Operations, Washington DC, Final Report, June 1974, DTIC AD-531 378.

11. *MPS Users Manual*, WinMPS Version 95-01, Kaman Sciences Corporation, 30 September 1995.

12. Regan, Frank J., *Re-Entry Vehicle Dynamics*, American Institute of Aeronautics and Astronautics, Inc., New York, 1984.

13. Robbins, Jack B., *Operational Limitations on MIRV Fractionation*, Student Report,
    Air Command and Staff College, Air University, April 1985,
    DTIC AD-B093 075.

14. Wiesel, W., Author of *Space Dynamics*, Personal Interview, 30 October, 1996.

Vita

Major Elliot T. Fair was born on 4 January 1963 in Bennington VT. He graduated from Salem High School, Salem NH in 1981 and attended the United States Air Force Academy in Colorado Springs, CO, graduating with a Bachelor's of Science in Astronautical Engineering. After completing Undergraduate Pilot Training, he flew B-52G's at Griffiss AFB NY. In 1989 he was selected to pilot the B-1B Lancer. During his tour at Dyess AFB, TX, he served as a B-1B Aircraft Commander, Instructor Pilot, RTU Instructor Pilot, and RTU Stan Eval Instructor Pilot. He entered the Graduate School of Engineering, Air Force Institute of Technology, in August 1995.

Permanent Address: 17 Glen Denin Dr

Salem, NH 03079

REPORT DOCUMENTATION PAGE

Form Approved
OMB No. 0704-0188

1. AGENCY USE ONLY *(Leave blank)*	2. REPORT DATE February 1997	3. REPORT TYPE AND DATES COVERED Master's Thesis

4. TITLE AND SUBTITLE

Adding MIRV Footprint Constraints to the Weapons Assignment Model

5. FUNDING NUMBERS

6. AUTHOR(S)

Elliot T. Fair, Major, USAF

7. PERFORMING ORGANIZATION NAME(S) AND ADDRESS(ES)

Air Force Institute of Technology/ENS
2750 P Street
Wright-Patterson AFB, Ohio 45433-7765

8. PERFORMING ORGANIZATION REPORT NUMBER

AFIT/GOA/ENS/97-04

9. SPONSORING / MONITORING AGENCY NAME(S) AND ADDRESS(ES)

USSTRATCOM/J533
901 SAC BLVD
OFFUTT AFB, NE 68113-6500

10. SPONSORING / MONITORING AGENCY REPORT NUMBER

11. SUPPLEMENTARY NOTES

12a. DISTRIBUTION / AVAILABILITY STATEMENT

Approved for Public Release; Distribution is Unlimited

12b. DISTRIBUTION CODE

13. ABSTRACT *(Maximum 200 words)*

US Strategic Command (USSTRATCOM) is developing a new linear programming model called the Weapons Assignment Model (WAM) to perform weapons assignment for the Strategic Integrated Operations Plan (SIOP). One of the major improvements WAM will have over its predecessor is the ability to include Multiple Indepenently Targetable Reentry Vehicle (MIRV) footprinting constraints in the optimization process. In order to include MIRV footprint constraints in WAM, a methodology is needed to model the MIRV footprints in a manner that is consistent with the limitations of linear programming. Two techniques for modeling MIRV footprints were developed. The first, Geometric Approximation (GA), uses a carefully positioned and sized ellipse on the earth's surface to model the capabilities of a Post Boost Vehicle (PBV) to disperse MIRVs. Any combination of targets within the ellipse is considered to constitute a feasible targeting plan for a missile. The second model is called Energy Space Transformation (EST). This model scales the distance each MIRV is displaced from the missile aimpoint to account for the PBV energy required to maneuver for each MIRV. The sum of the maneuvering energy for each MIRV is used to calculate the fraction of the PBV energy required to strike a particular combination of targets. Any combination where the fraction is less than one is considered feasible. These two models were tested and validated using 120 missile sorties. Both models were approximately 85 percent accurate.

14. SUBJECT TERMS

MIRV, Footprint, Weapons Assignment Model, Arsenal Exchange Model;

15. NUMBER OF PAGES
114

16. PRICE CODE

17. SECURITY CLASSIFICATION OF REPORT Unclassified	18. SECURITY CLASSIFICATION OF THIS PAGE Unclassified	19. SECURITY CLASSIFICATION OF ABSTRACT Unclassified	20. LIMITATION OF ABSTRACT UL

GENERAL INSTRUCTIONS FOR COMPLETING SF 298

The Report Documentation Page (RDP) is used in announcing and cataloging reports. It is important that this information be consistent with the rest of the report, particularly the cover and title page. Instructions for filling in each block of the form follow. It is important to *stay within the lines* to meet *optical scanning requirements*.

Block 1. Agency Use Only *(Leave blank)*.

Block 2. Report Date. Full publication date including day, month, and year, if available (e.g. 1 Jan 88). Must cite at least the year.

Block 3. Type of Report and Dates Covered. State whether report is interim, final, etc. If applicable, enter inclusive report dates (e.g. 10 Jun 87 - 30 Jun 88).

Block 4. Title and Subtitle. A title is taken from the part of the report that provides the most meaningful and complete information. When a report is prepared in more than one volume, repeat the primary title, add volume number, and include subtitle for the specific volume. On classified documents enter the title classification in parentheses.

Block 5. Funding Numbers. To include contract and grant numbers; may include program element number(s), project number(s), task number(s), and work unit number(s). Use the following labels:

C	-	Contract	PR	- Project
G	-	Grant	TA	- Task
PE	-	Program Element	WU	- Work Unit Accession No.

Block 6. Author(s). Name(s) of person(s) responsible for writing the report, performing the research, or credited with the content of the report. If editor or compiler, this should follow the name(s).

Block 7. Performing Organization Name(s) and Address(es). Self-explanatory.

Block 8. Performing Organization Report Number. Enter the unique alphanumeric report number(s) assigned by the organization performing the report.

Block 9. Sponsoring/Monitoring Agency Name(s) and Address(es). Self-explanatory.

Block 10. Sponsoring/Monitoring Agency Report Number. *(If known)*

Block 11. Supplementary Notes. Enter information not included elsewhere such as: Prepared in cooperation with...; Trans. of...; To be published in.... When a report is revised, include a statement whether the new report supersedes or supplements the older report.

Block 12a. Distribution/Availability Statement. Denotes public availability or limitations. Cite any availability to the public. Enter additional limitations or special markings in all capitals (e.g. NOFORN, REL, ITAR).

DOD - See DoDD 5230.24, "Distribution Statements on Technical Documents."
DOE - See authorities.
NASA - See Handbook NHB 2200.2.
NTIS - Leave blank.

Block 12b. Distribution Code.

DOD - Leave blank.
DOE - Enter DOE distribution categories from the Standard Distribution for Unclassified Scientific and Technical Reports.
NASA - Leave blank.
NTIS - Leave blank.

Block 13. Abstract. Include a brief *(Maximum 200 words)* factual summary of the most significant information contained in the report.

Block 14. Subject Terms. Keywords or phrases identifying major subjects in the report.

Block 15. Number of Pages. Enter the total number of pages.

Block 16. Price Code. Enter appropriate price code *(NTIS only)*.

Blocks 17. - 19. Security Classifications. Self-explanatory. Enter U.S. Security Classification in accordance with U.S. Security Regulations (i.e., UNCLASSIFIED). If form contains classified information, stamp classification on the top and bottom of the page.

Block 20. Limitation of Abstract. This block must be completed to assign a limitation to the abstract. Enter either UL (unlimited) or SAR (same as report). An entry in this block is necessary if the abstract is to be limited. If blank, the abstract is assumed to be unlimited.